NASA Technical Memorandum 86398

Ground Vibration Test of the Laminar Flow Control JetStar Airplane

Michael W. Kehoe, F. W. Cazier, Jr.,
and Joseph F. Ellison

OCTOBER 1985

NASA Technical Memorandum 86398

Ground Vibration Test of the Laminar Flow Control JetStar Airplane

Michael W. Kehoe
Ames Research Center
Dryden Flight Research Facility
Edwards, California

F. W. Cazier, Jr.
Langley Research Center
Hampton, Virginia

Joseph F. Ellison
Ames Research Center
Dryden Flight Research Facility
Edwards, California

National Aeronautics
and Space Administration

**Scientific and Technical
Information Branch**

1985

Summary

A ground vibration test was conducted on a Lockheed JetStar airplane that had been modified for the purpose of conducting laminar flow control experiments. Wing modifications included removal of external wing fuel tanks, installation of a different laminar flow control leading-edge test section on each wing, and closing the gap in the trailing-edge flaps. The ground vibration test was conducted by using sine-dwell and single-point-random excitation. The test was performed prior to initial flight flutter tests to determine the mode frequencies, mode shapes, and structural damping coefficients. The data presented include frequency response functions and a comparision of mode frequencies and mode shapes from both methods.

Introduction

Laminar Flow Control (LFC) technology is being developed because of its potential for reducing wing drag and improving fuel economy. Laminar flow is obtained by incorporating a suction system near the wing leading edge to remove some of the boundary-layer air. Removing a portion of this low-energy air keeps the airflow attached to the surface and delays the onset of turbulent, separated airflow. Laminar flow produces a smooth layer of air over much more of the wing than would be experienced by a traditional airfoil and significantly reduces the drag induced by turbulent boundary-layer air. The NASA program to demonstrate LFC leading-edge test sections is called LEFT for Leading-Edge Flight Test Program.

In order to demonstrate the effectiveness of LFC under flight conditions representative of commercial transport cruise operation, a Lockheed JetStar airplane was extensively modified. Wing modifications included removal of the external fuel slipper tanks and installation of leading-edge test sections designed by the Lockheed-Georgia Company and the Douglas Aircraft Company for the left and right wings, respectively. Upper and lower wing fairings aft of these devices complete the test sections. The Douglas design includes a Krueger flap or shield which is deployed at low speeds and altitudes. The gap in the trailing-edge flap left by the tank removal was closed. The leading-edge flaps were fixed and the leading-edge fuel bays were empty.

In preparation for initial flight tests, a ground vibration test (GVT) was conducted on the LFC JetStar. The GVT was conducted to identify and define the structural modes of the airplane. This information provides the dynamic definition of the structure which can be used for such things as upgrading structural models and assessing the validity of flutter analyses. The tests were performed by using both sine-dwell and single-point-random excitation methods.

The sine-dwell phase of the test was a joint effort of the Langley Research Center and the Dryden Flight Research Facility of the Ames Research Center (Ames-Dryden). The Lockheed-Georgia Company provided technical assistance. Three 12-hour days were required to acquire the data for this phase of the test. The single-point-random phase of the test was conducted by Ames-Dryden. One 12-hour day was required to complete this phase of the test.

The sine-dwell method was considered the primary method for this test. It is regarded as the standard method against which other methods are compared. The random excitation method has the advantage of allowing a GVT to be conducted in shorter time but it requires computer analysis of the data.

The tests were conducted at Ames-Dryden from October 27, 1983 through November 2, 1983. The objectives of the tests were

1. To identify airplane structural modes and frequencies for modes up to 45 Hz
2. To measure symmetric and antisymmetric wing mode shapes, node lines, frequencies, and damping to 24 Hz
3. To compare results obtained from sine-dwell and single-point-random excitation.

Airplane Configuration

The test airplane for demonstrating Laminar Flow Control is NASA 814. Figure 1 shows the location from which the external fuel tanks were removed and indicates the trailing-edge modification (mod). The two different leading-edge test sections and their associated fairings are shown on the left and right wings.

The left-wing leading-edge test section was attached to the forward spar. This device has fine spanwise slots on both upper and lower surfaces from the leading edge to the front spar. A titanium outer skin is bonded to a sandwich substructure of graphite-epoxy face sheets with a Du Pont Nomex honeycomb core. A cross-sectional view and the basic dimensions are shown in figure 2.

The right-wing leading-edge test section was attached through ribs to the front spar. This device consists of a suction panel made of an electronic-beam-perforated titanium skin and bonded to a corrugated fiberglass substructure. A retractable Krueger flap was extended from the lower surface of the test section to shield the porous leading edge during flights below test altitudes. The flap was designed to provide very little lift to minimize asymmetric aerodynamic effects of an extended flap on one side only. Figure 3 gives its basic dimensions and a cross-sectional view.

The airplane was structurally asymmetric since the two laminar flow control devices were different in construction. However, the weight of each section was approximately the same and, therefore, similar structural response on the left and right wing was expected. The left and right middle leading-edge flap sections were removed to accommodate the

test sections. The outboard and inboard leading-edge flap sections were locked. The flap modifications are shown in figure 4. More detailed information on the airplane modifications can be found in reference 1.

The ground vibration test (GVT) was conducted in the Flight Loads Research Facility at Ames-Dryden. The overall test setup is shown in figure 5. (The pylon on the top of the fuselage is a NASA test fixture from previous tests.) The airplane was supported on its landing gear during the test. The landing-gear struts were collapsed to eliminate potential nonlinear oscillations of the oleo strut. The struts were actually compressed onto wood blocks which had been inserted to prevent damage to the struts (fig. 6). The tires were deflated to 100 psi (approximately one-half the normal pressure) to provide a soft support.

The wing fuel tanks were empty. Airplane electrical and hydraulic power was applied during the initial testing but was discontinued after it was determined to have little effect on the wing modal frequencies and shapes. The control surface rotation modes were examined with and without hydraulic power.

Test Equipment

The GVT was conducted by using both sine-dwell and single-point-random excitation techniques. Some equipment was common to both methods, whereas additional equipment was unique to each method. The 150-lbf electrodynamic shakers and piezoelectric accelerometers were common to both methods. The shakers with current feedback and individual gain and phase control are used to input a forcing function to the structure. The accelerometers were attached to the airplane to measure the response of the structure. The accelerometer signal was amplified by a remote preamplifier and by a signal conditioning amplifier.

Sine-Dwell Equipment

The sine-dwell GVT equipment was housed in two portable consoles, one of which is shown in figure 7. The system was capable of acquiring, filtering, displaying, and recording six channels of accelerometer data. Two shakers were used to input a sinusoidal forcing function to the structure. The amplified accelerometer signals were filtered with tracking filters with a 2.0-Hz bandwidth. A patch panel was utilized to route the signal to several common display and recording devices. A coincident/quadrature (co-quad) analyzer is part of this system.

Single-Point-Random Equipment

The minicomputer-based GenRad model 2508 structural analysis system used for the GVT is housed in one portable console as seen in figure 8. The system was capable of acquiring, filtering, displaying, and recording four channels of data (one input and three responses). The system operates by exciting the airplane through one of the previously described shakers with either a sinusoidal or a random forcing function and analyzing the resultant vehicle response.

Test Procedures

Sine-Dwell Excitation

Two shakers were used to excite the airplane rigid-body and elastic modes, whereas control surface rotation frequencies were determined with a single shaker. The locations on the airplane at which shakers were attached are listed in table I. Each shaker was attached to the airplane by means of a telescoping thrust rod, a mechanical fuse, and a force link. These components are shown in figure 9. The fuse attached to a locking ball nut joint which was either mounted directly to the structure by a threaded stud or bonded to the structure.

Frequency sweeps. The frequency sweeps were generally from 1 to 45 Hz. A logarithmic sweep rate of 0.5 decade/min was used. Accelerometers were placed at several locations and in various orientations. The frequency response plots of these accelerometers were recorded on the X-Y plotters. These plots indicate frequencies of significant structural response on each structural component.

Structural mode measurements. After the frequency sweeps were completed, each aircraft structural mode was fine-tuned by using a co/quad analyzer with one acceleration and one force signal as inputs. Each mode was tuned by minimizing the coincident (in-phase) component and maximizing the quadrature (out-of-phase) component of the signal. Records of acceleration versus time were also used to verify phasing between the left and right sides of the airplane. Another check on the purity of the mode was to terminate electrical power to the shaker and observe the decay of the oscillations for beats. The absence of beats in the decay trace indicates that a mode is properly tuned.

Most of the accelerometer locations which were on the airplane for measuring structural modes are shown in figure 10. (Points not shown are 45-46, 55, 83-90, 60-61, 72, and 74 which mirror points 9-10, 19, 75-82, 24-25, 34, and 36, respectively, on the right side. Points 63 and 64 are on the Krueger flap.) Wooden blocks (fig. 11) shaped to the contour of the surface were glued to wing and fuselage locations to facilitate vertical and lateral measurements and to insure that the vertical accelerations measured were normal to the ground. Vertical accelerations were measured at the points on the wing, fuselage, engine nacelles, and horizontal tail. Lateral accelerations were measured on the vertical tail and along the fuselage. Fore-and-aft accelerations were also measured at the wingtip points 26 and 47.

Once a mode was tuned, a modal survey was performed with the roving accelerometers. The point on the structure with the largest amplitude was selected as the reference point. The reference was used to normalize all other accelerometer response values and to determine phase relationships with

roving accelerometers. Each roving accelerometer was placed at the reference point before a survey to compare amplitude readings. The accelerometer amplifier gains were adjusted as necessary to insure uniform readings. Most of the survey locations could be reached by hand. Figures 12 and 13 show the accelerometer on a wand which was used to reach the remaining points. Some modes were surveyed completely while other modes were surveyed only to the extent that the type mode could be identified. In general, the survey included both the left and right sides of the airplane.

Single-Point-Random Excitation

References 2 and 3 describe the single-point-random excitation and data analysis method. Briefly, the system first generates a random forcing function of a bandwidth and amplitude specified by the user. The forcing function time history is then recorded on a tape recorder. Following this, the signal was played back through the electrodynamic shaker attached to the airplane. The input force spectrum used is shown in figure 14. A schematic of the test setup is shown in figure 15. The single shaker was attached to the left wingtip at the aft spar.

Data were acquired with the structural analysis system at each of the 93 locations used for the sine-dwell test. Three accelerometer signals and the reference input force were input into the analyzer. Transfer and coherence functions were then calculated. The coherence function was used as a measurement of the quality of the data before it was stored on the system disk. The baseband data were sampled at 128 samples per second using a data block size of 1024 samples. The antialiasing filters were set at 50 Hz. The total number of averages used to calculate each transfer function was 300. A Hanning window was used to reduce leakage errors. In the analysis of random excitation, all modes, symmetric and antisymmetric, were obtained at the same time. Because of the number of modes between 4 and 12 Hz, it was necessary to increase the frequency response function resolution in this bandwidth (by using a zoom transform) to provide sufficient resolution to estimate the modal parameters.

Once data acquisition was completed for the entire airplane, frequency, damping, phase, and amplitude were estimated for each mode by fitting a multidegree-of-freedom curve to a selected transfer function that exhibited a good response for the structural modes of interest. The estimated modal parameters, particularly phase, for each mode were examined to determine if the curve fit was acceptable. It was necessary to examine several transfer functions to insure a good curve fit for all the structural modes below 50 Hz.

Once a good fit was obtained to estimate the modal parameters (frequency, damping, amplitude, and phase), the modal coefficients for each mode shape were calculated at all points by using the amplitude and phase of the measured response at the selected resonance frequency. Animated mode shapes were then displayed to identify each mode.

Results and Discussion

Rigid-Body Modes

The frequency and structural damping of the rigid-body modes of the airplane supported on its landing gear were measured. These modes included pitch, yaw, and roll. Vertical translation could not be excited. No attempt was made to determine fore-and-aft or lateral translation. The measured rigid-body frequencies are as follows:

Mode	Frequency, Hz	Structural Damping
Yaw	1.20	0.047
Pitch	2.45	0.044
Roll	3.62	0.021

Structural Modes

Frequency response functions. Single and multiple shaker frequency sweeps were performed at several force levels and with shakers at several locations on the airplane. Symmetric and antisymmetric sweeps were performed to identify approximate frequencies of modes and to insure that modes were not omitted. The control surface rotation frequencies and the Krueger flap frequencies were determined by single shaker sweeps. Seventeen sweeps were performed. These data are presented in appendix A.

The frequency response functions which were obtained from the single-point-random excitation are analogous to the frequency sweeps obtained during the sine excitation portion of the GVT except that all symmetric and antisymmetric modes are present at the same time. The random excitation frequency response functions are presented in appendix B.

Mode Identification. Structural modes were identified by their mode shapes and frequencies. Table II lists the measured frequencies of the LFC JetStar modes that were identified both by the sine-dwell and the single-point-random methods. Also listed in this table, for comparison, are the measured frequencies of a standard (empty fuel) JetStar GVT performed by Lockheed in 1961 (ref. 4). The 1961 test data were used only as an additional check to verify mode identification and to assure that no modes were overlooked. A complete or partial mode survey was made for each of the modes identified in the table. Appendix C presents each of the mode shapes determined by the two test methods.

Comparison of Results From Two Methods

Structural modes. There was good agreement between the frequency values obtained from the two methods. The frequency values extracted by the random excitation technique were slightly higher in value for all but one of the modes identified. These frequency values may have been higher because of the differences in force level between the

sine-dwell and single-point-random excitation techniques. One mode, the 7.90 Hz empennage yaw with fuselage side bending, was determined only by the single-point-random method. Since this was not a wing mode, no attempt was made to excite it during the sine-dwell portion of the test.

A comparison of damping values indicated that the values obtained from random excitation were generally lower than those obtained from the sine-dwell method. The three exceptions were the 4.90, 7.49, and 16.12 Hz symmetric modes.

A comparison of the mode shape data (appendix C) in general indicated good agreement. It should be noted that for the random excitation, the right wing of the airplane responded differently than the left wing for some of the structural modes. A review of the frequency response functions (appendix B) obtained from the random excitation revealed that, above 10 Hz, several modes were not well excited on the right wing. This was most likely due to a single shaker providing the excitation at the left wingtip and therefore not providing an even distribution of energy to the airplane. This lack of excitation on the right wing could also be due to the effects of the landing gear on the airplane response. Only one shaker location (left wing) was used for random excitation for this test. Other shaker locations would be needed to insure a better energy distribution and better excitation of all the structural modes of interest. The engine nacelles and horizontal stabilizer were fairly symmetric in response between the right and left sides.

The wing torsion modes were difficult to excite. The shakers were moved inboard on the rear spar of the wing to excite the torsion mode with sine excitation. The response of the symmetric torsion mode was asymmetric in that each wing was tuned at a different frequency (table II). Only the symmetric torsion mode for the right wing was excited with single-point-random excitation. The left-wing torsion mode was not excited by this method because of the shaker location. The wingtip shaker location was identical for both methods of excitation. This mode was probably not excited by the random excitation because of insufficient energy at this frequency.

Control surface modes. The control surface rotation frequencies were determined by using sine-dwell excitation. Sweeps were conducted with hydraulic pressure on and off and at different force levels. These data are presented in appendix A. Aileron amplitude with hydraulic power on was higher but the frequencies were the same. No effort was made to preload the control surfaces to remove the free play. The free play in the ailerons and elevators was small, whereas the trailing-edge flaps exhibited noticeable free play. The measured control surface rotation frequencies are presented in table III. Two Krueger flap modes at 40 and 46 Hz were obtained by shaking with a single shaker on the extended Krueger flap.

Concluding Remarks

Prior to initial flight tests, a ground vibration test was conducted on a Lockheed JetStar airplane that had been extensively modified for a Laminar Flow Control Program. Wing modifications of significance included removal of the wing fuel slipper tanks and the installation of a laminar flow control test section on each wing. Additionally, the resultant gap in the trailing-edge flaps was faired in and the leading-edge fuel bays were emptied.

For the ground vibration test, the airplane was supported on its landing gear with reduced air pressure in the tires. The test was conducted by using both sine-dwell and single-point-random excitation methods. Rigid-body, wing control surface, and structural modes were identified. Both test methods were effective. The modal frequencies obtained from the random excitation were slightly higher than the frequency values obtained from the sine-dwell method. The structural damping values obtained from the random excitation, in general, were lower than the values determined by the sine-dwell method. The right- and left-wing response was not the same for some of the structural modes when excited by the single-point-random method. This may reflect an inadequate excitation of the airplane on the side opposite the shaker. Repositioning the shaker to the other side should eliminate this lack of symmetry.

The free play in the ailerons and elevators was small, whereas the trailing-edge flaps exhibited noticeable free play. With the Krueger flap extended, its lowest flap mode was 40 Hz.

One anomaly observed was that the right and left wings exhibited symmetric first wing torsion modes at different frequencies. The antisymmetric first wing torsion mode frequency was the same for both wings; however, the antisymmetric first wing torsion mode was not determined by the single-point-random method. No other unusual vibratory motion was observed during the ground vibration test.

NASA Langley Research Center
Hampton, VA 23665
May 30, 1985

TABLE I. ELECTRODYNAMIC SHAKER LOCATIONS

Shaker	Location
Single	Leading-edge Krueger flap Left inboard trailing-edge flap Left outboard trailing-edge flap Left aileron
Two	Left and right wingtip rear spar at points[a] 11 and 47 Left and right wingtip front spar at points 1 and 37 Left and right wing midspan rear spar inboard at points 14 and 50

[a]See figure 10 for point location.

TABLE II. COMPARISON OF GROUND VIBRATION TEST MODAL FREQUENCIES AND DAMPING

Sine dwell		Single point random		Mode description	Standard Jetstar GVT
Frequency, Hz	Damping, *G*	Frequency, Hz	Damping, *G*		Frequency, Hz
Symmetric modes					
4.90	0.018	4.92	0.020	1st wing bending	5.2
7.49	0.016	7.57	0.017	Engine pylon bending with wing and stabilizer bending	7.2
10.86	0.037	10.79	0.034	Stabilizer and fuselage vertical bending	10.7
13.88	0.016	13.92	0.012	Stabilizer and wing bending fuselage vertical bending, engine pylon pitch	13.9
16.12	0.059	16.32	0.075	2d wing bending, engine pylon pitch	16.2
23.56	0.045	24.73	0.036	Right wing torsion	22.0
31.00	0.072			Left wing torsion	
Antisymmetric modes					
5.05	0.026	5.20	0.014	Empennage roll, fuselage torsion	5.0
5.75	0.026	5.97	0.014	Empennage roll, fuselage torsion engine pylon bending	5.75
		7.90	0.024	Empennage yaw, fuselage side bending	
9.18	0.014	9.27	0.012	Vertical fin bending	8.65
11.05	0.075	11.25	0.032	1st wing bending	10.4
15.24	0.045	15.39	0.044	Wing bending, engine pylon pitch	15.4
23.48				Wing torsion	21.5

TABLE III. SINE-DWELL FREQUENCIES OF ADDITIONAL MODES

Frequency, Hz	Mode description
10.5	Nose boom
11.60	Inboard flap rotation
14.03, 20.6	Aileron rotation
20.0–20.9	Outboard flap rotation
40.0, 46.0	Krueger flap rotation

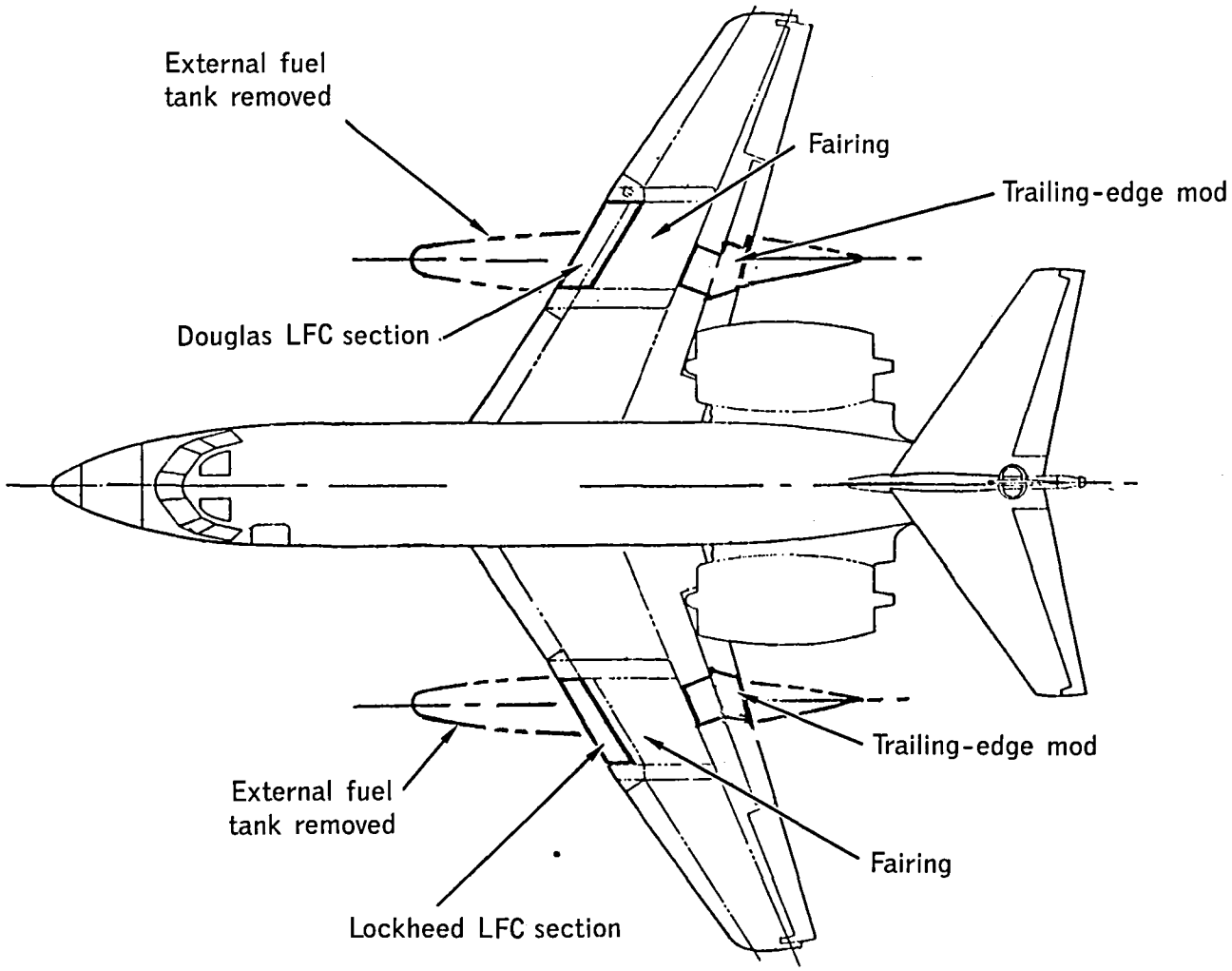

Figure 1. Laminar flow control JetStar modifications.

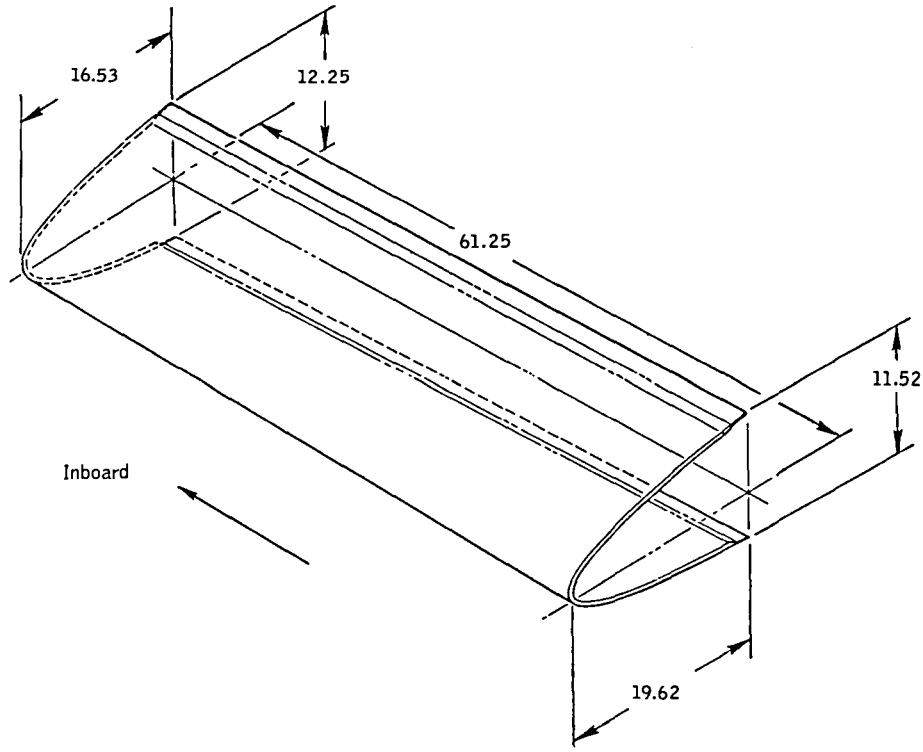

(a) Basic dimensions. All dimensions are in inches.

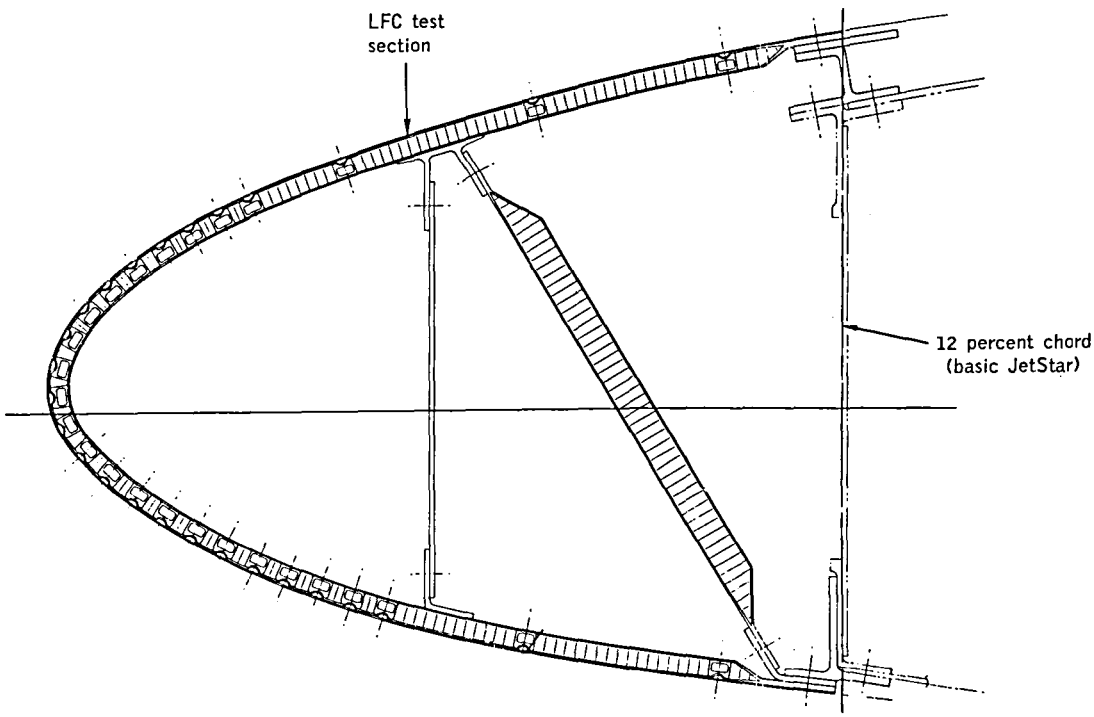

(b) Cross-sectional view.

Figure 2. Left-wing leading-edge test section.

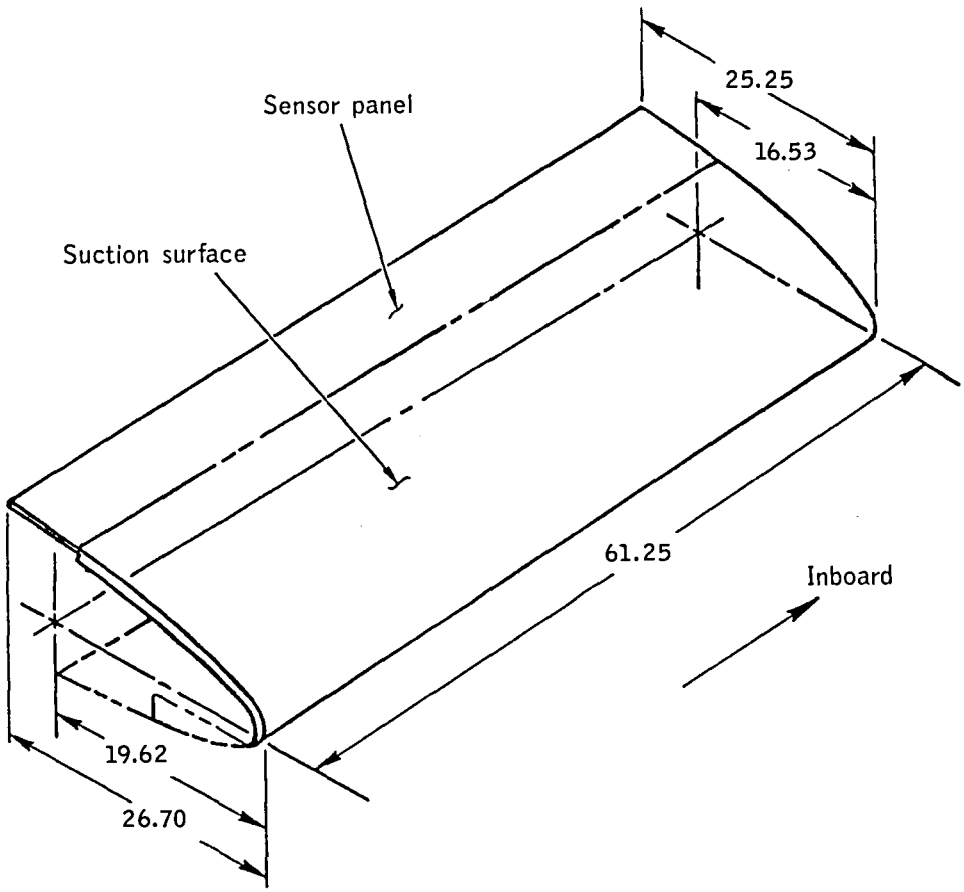

(a) Basic dimensions. All dimensions are in inches.

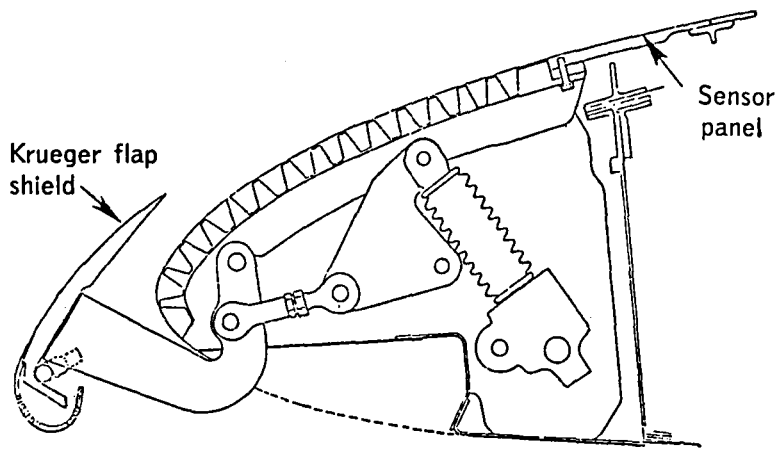

(b) Cross-sectional view (with Krueger flap extended).

Figure 3. Right-wing leading-edge test section.

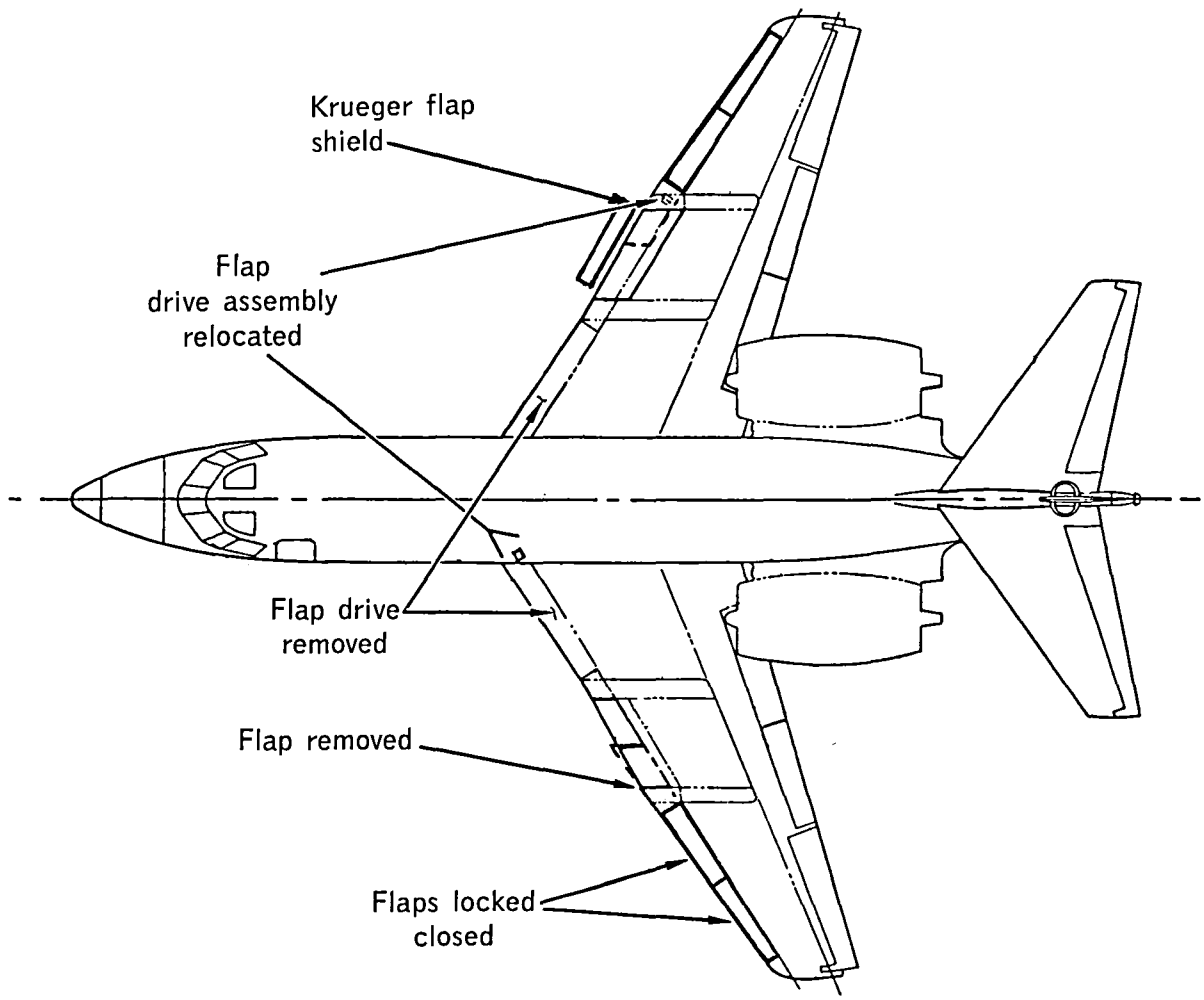

Figure 4. Leading-edge flap modification.

L-85-114

Figure 5. Airplane ground vibration test setup.

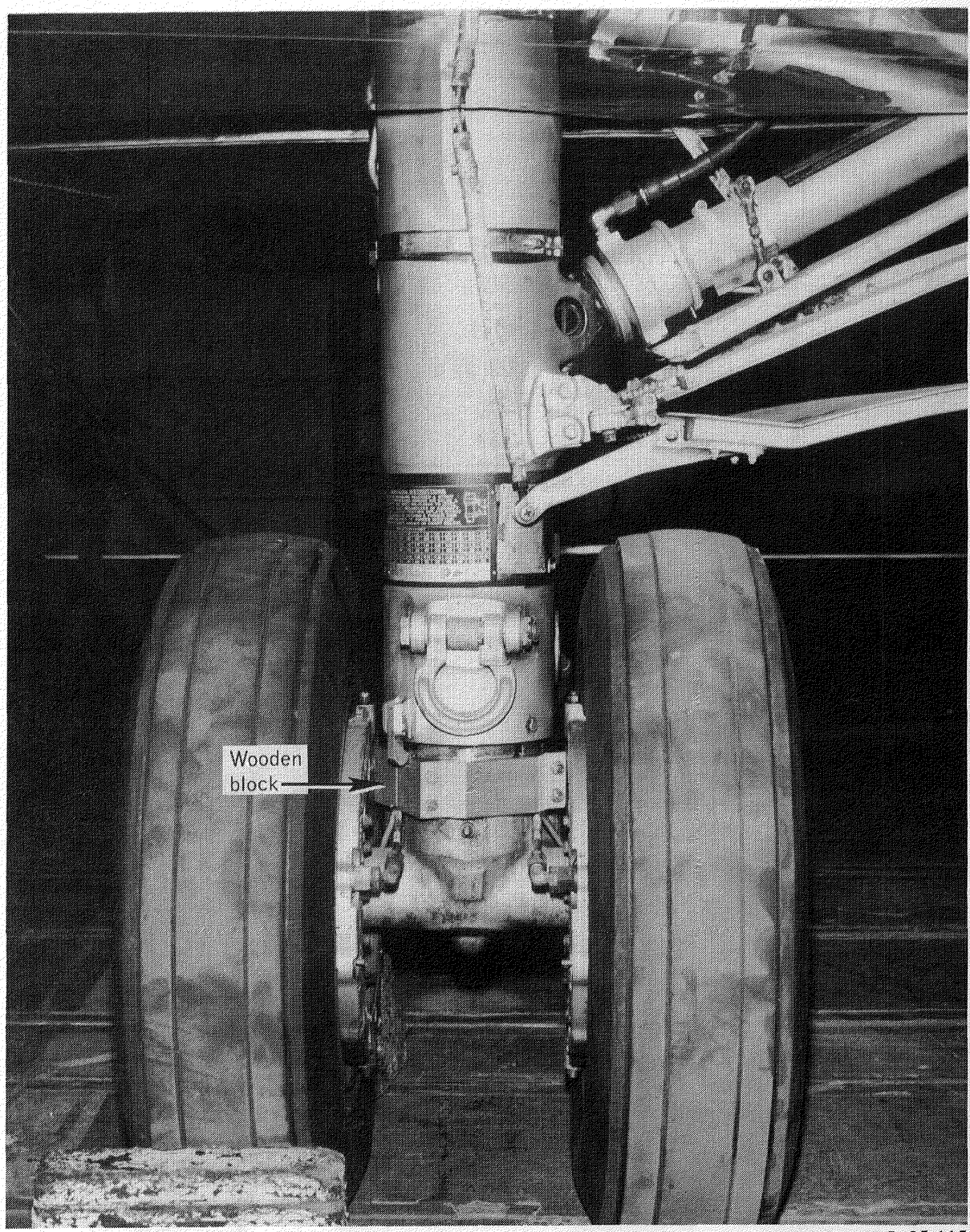

L-85-115

Figure 6. Main-landing-gear strut with wooden block inserted.

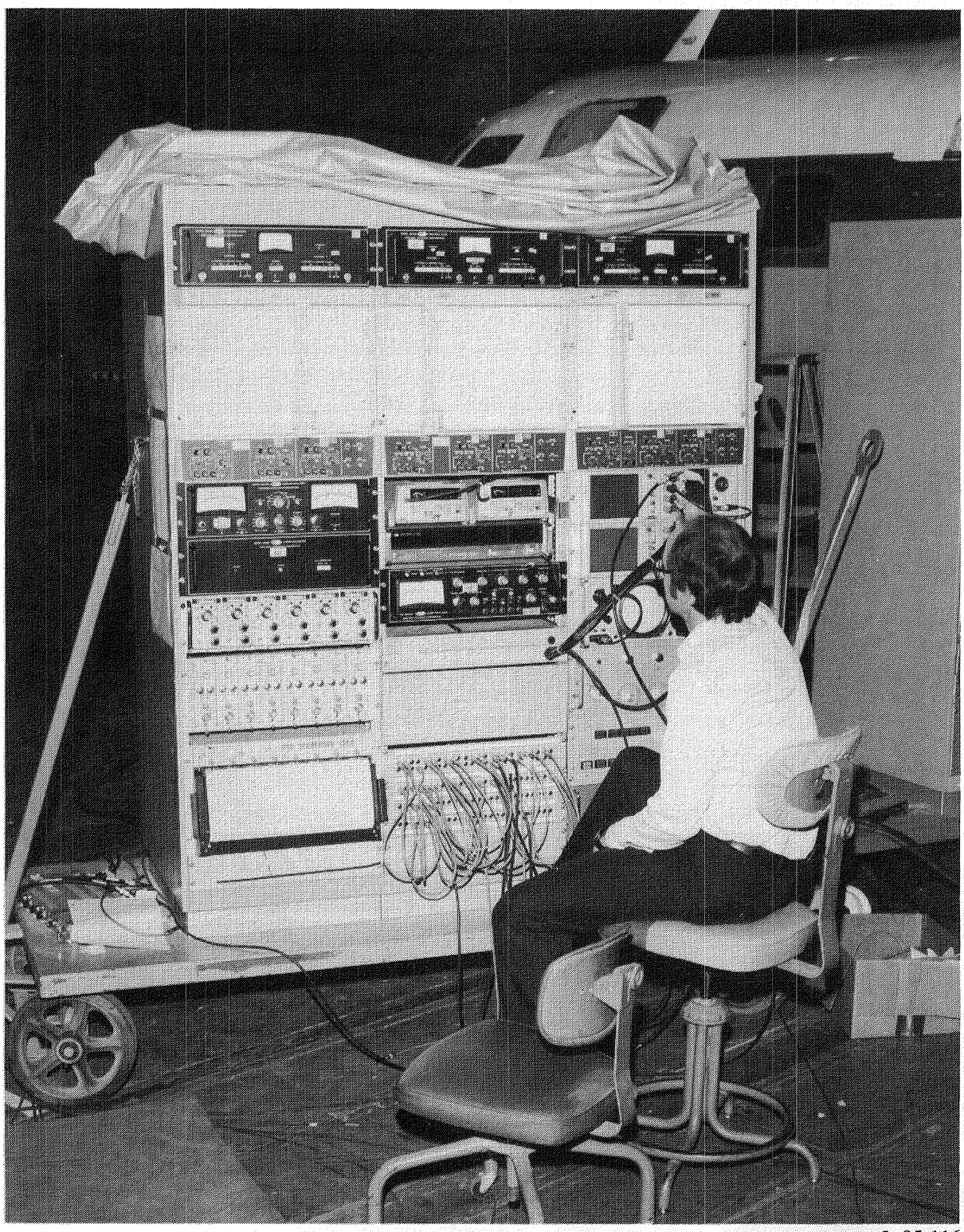

L-85-116

Figure 7. Sine-dwell ground vibration test equipment.

L-85-117

Figure 8. Minicomputer-based structural dynamics system.

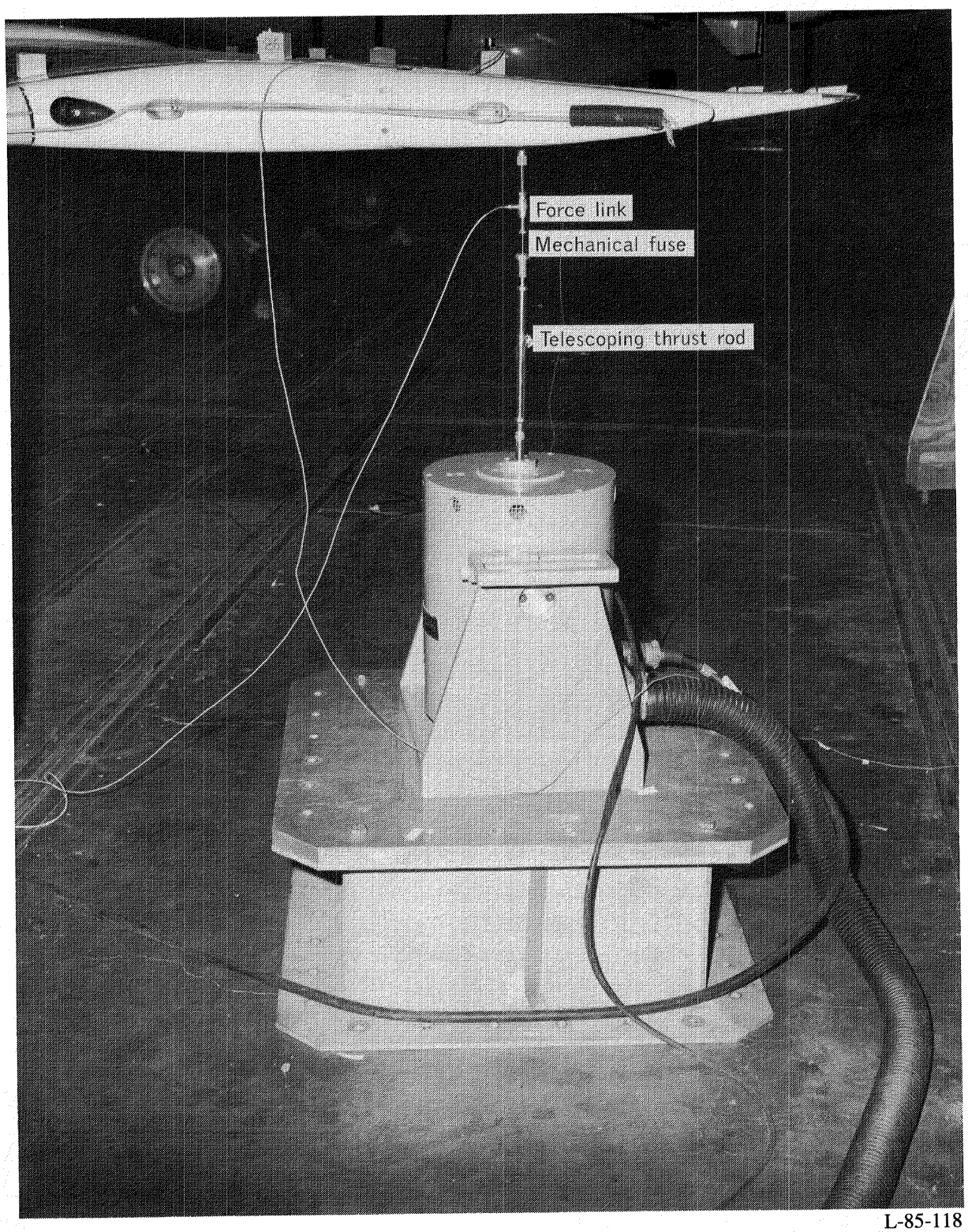

L-85-118

Figure 9. Electrodynamic shaker attachment on rear spar.

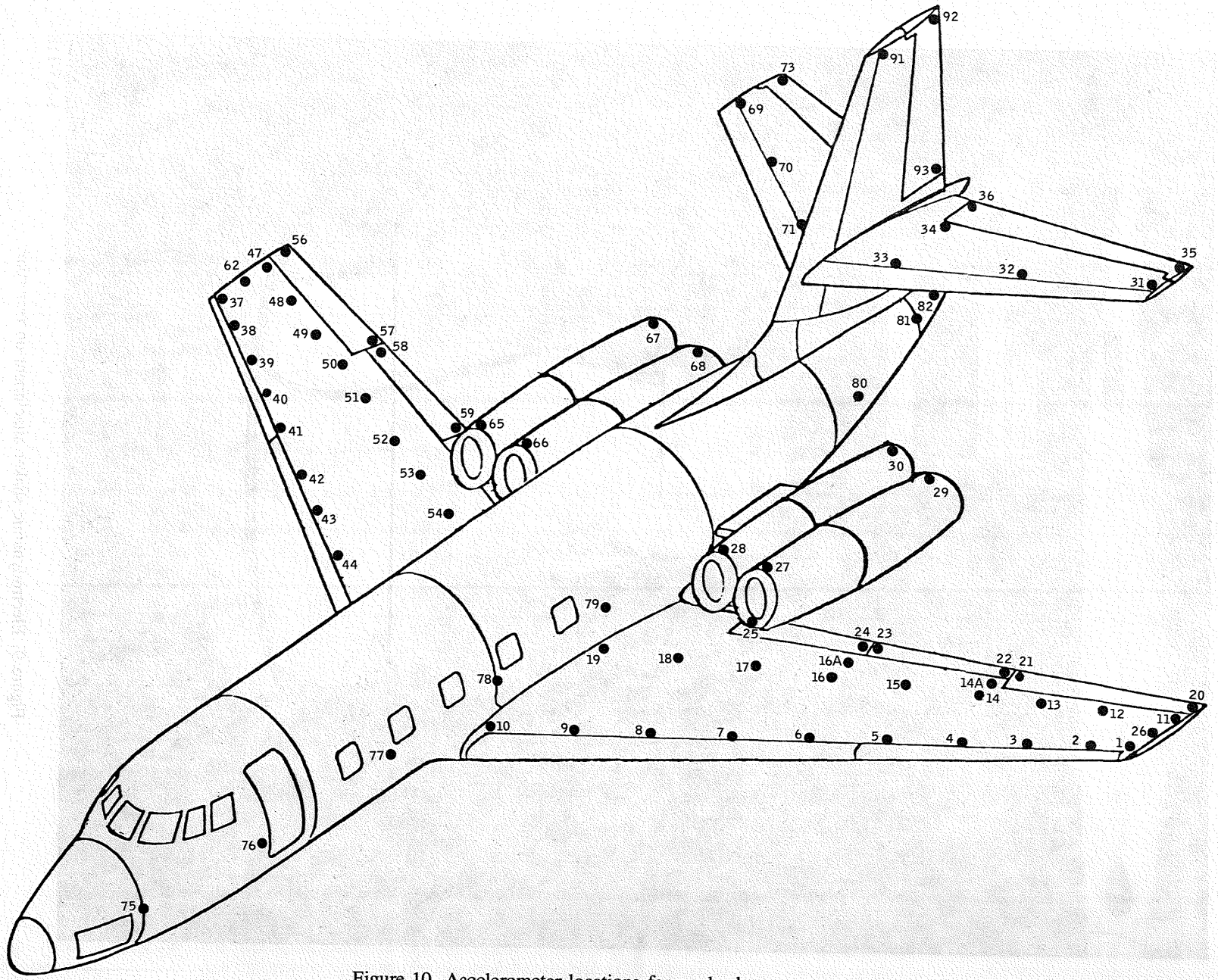

Figure 10. Accelerometer locations for mode-shape measurements.

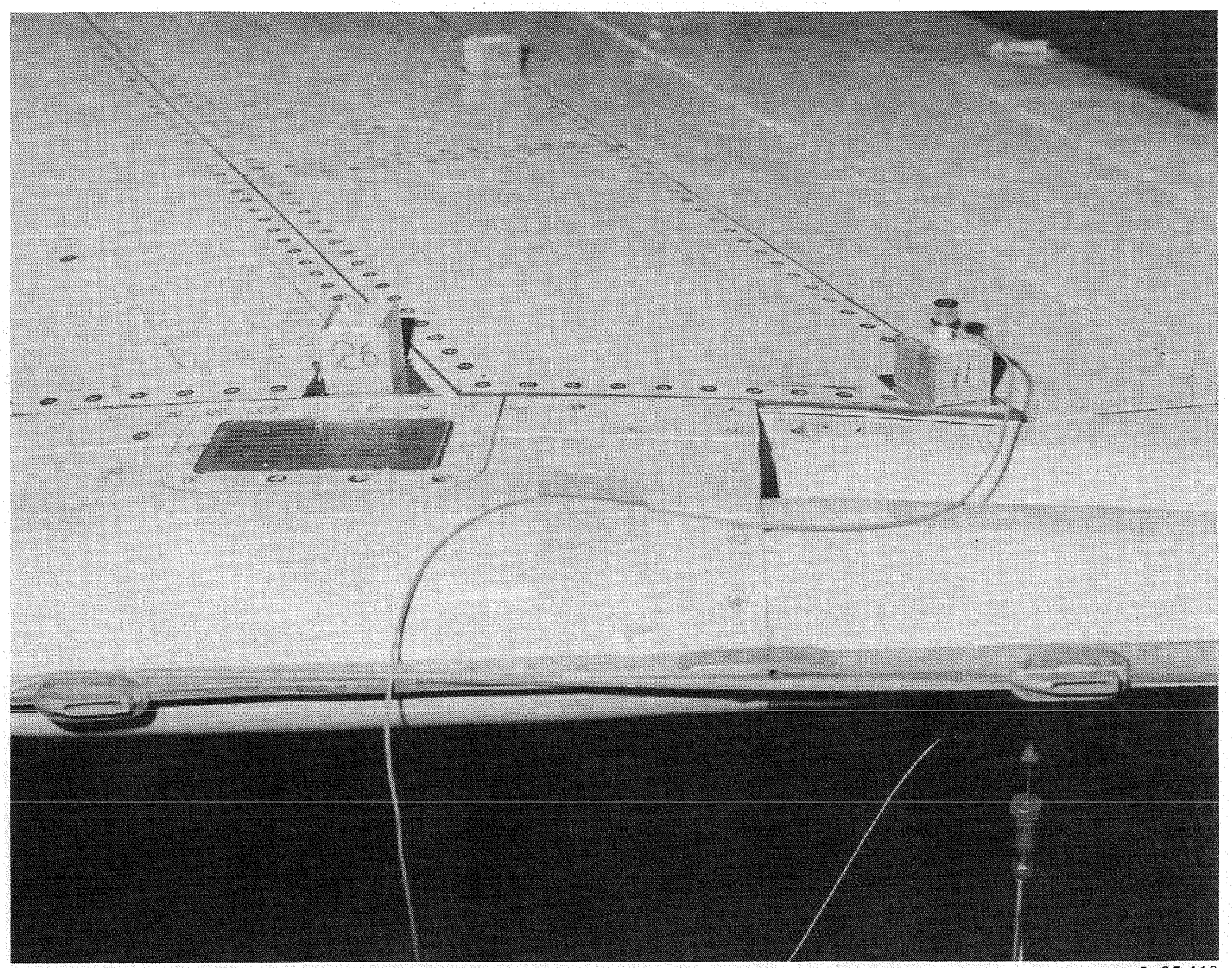

L-85-119

Figure 11. Wooden blocks for accelerometers.

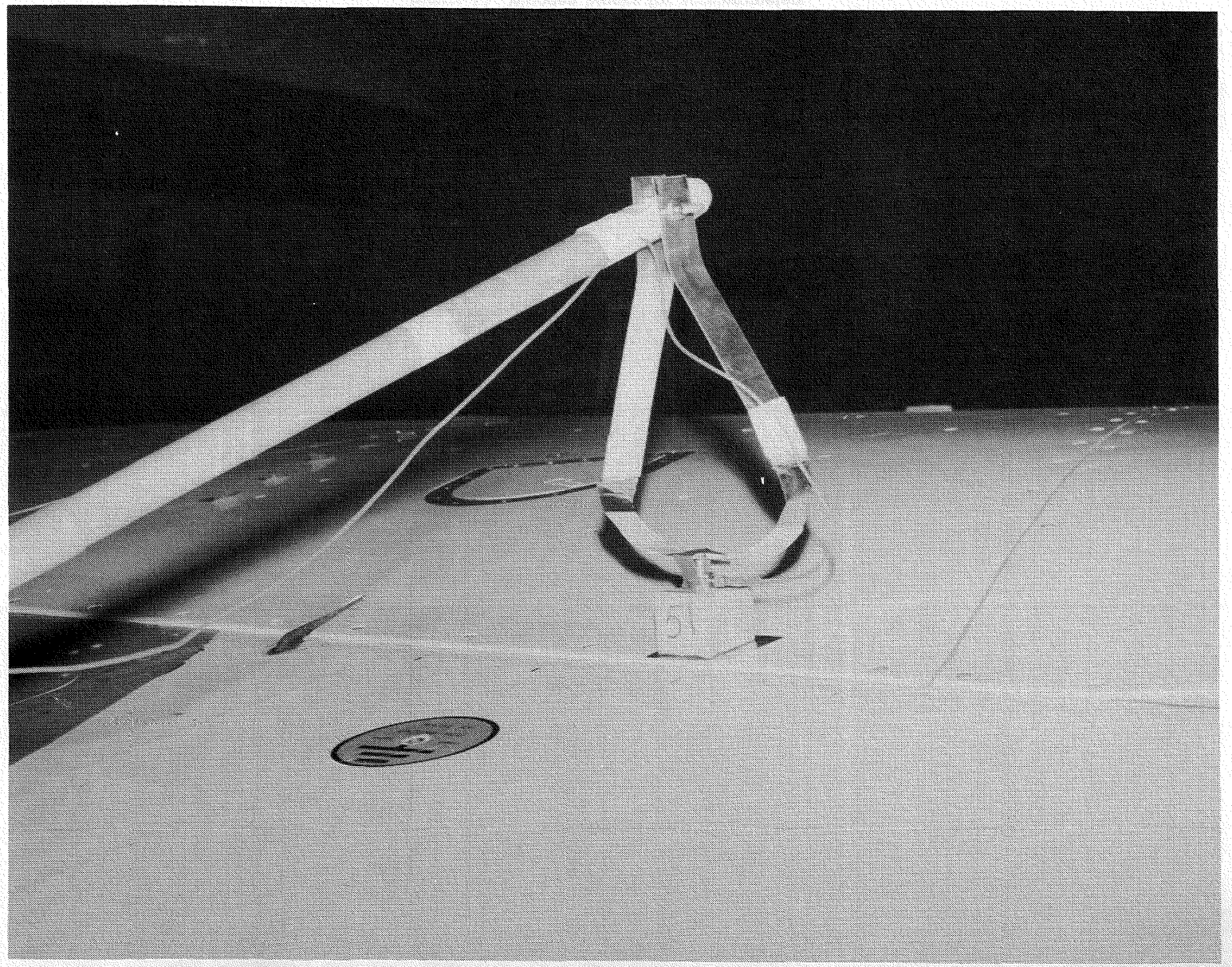

L-85-120

Figure 12. Accelerometer attached to a roving wand.

L-85-121

Figure 13. Roving wand being used to measure vertical tail motion.

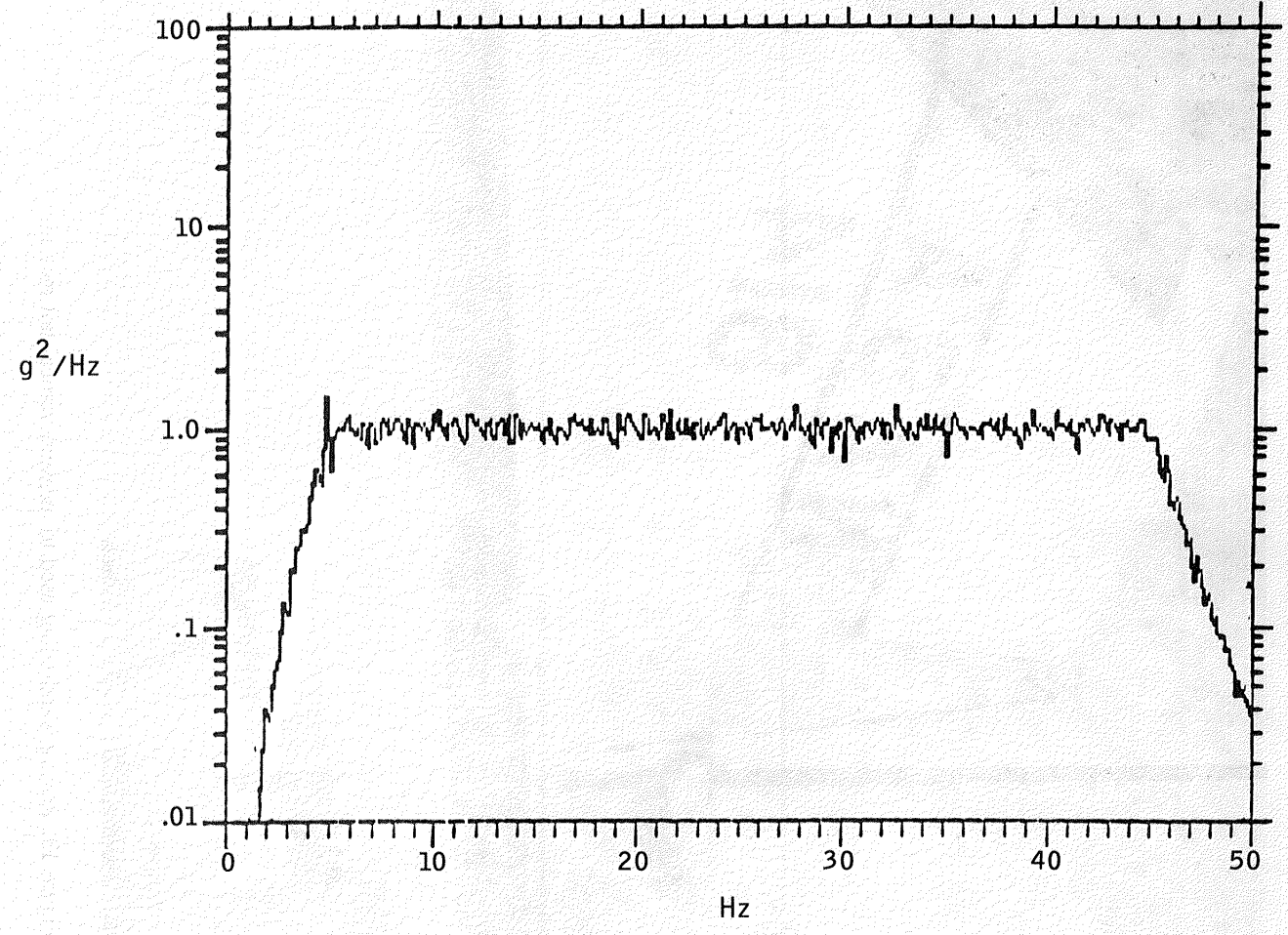

Figure 14. Single-point-random input force spectrum.

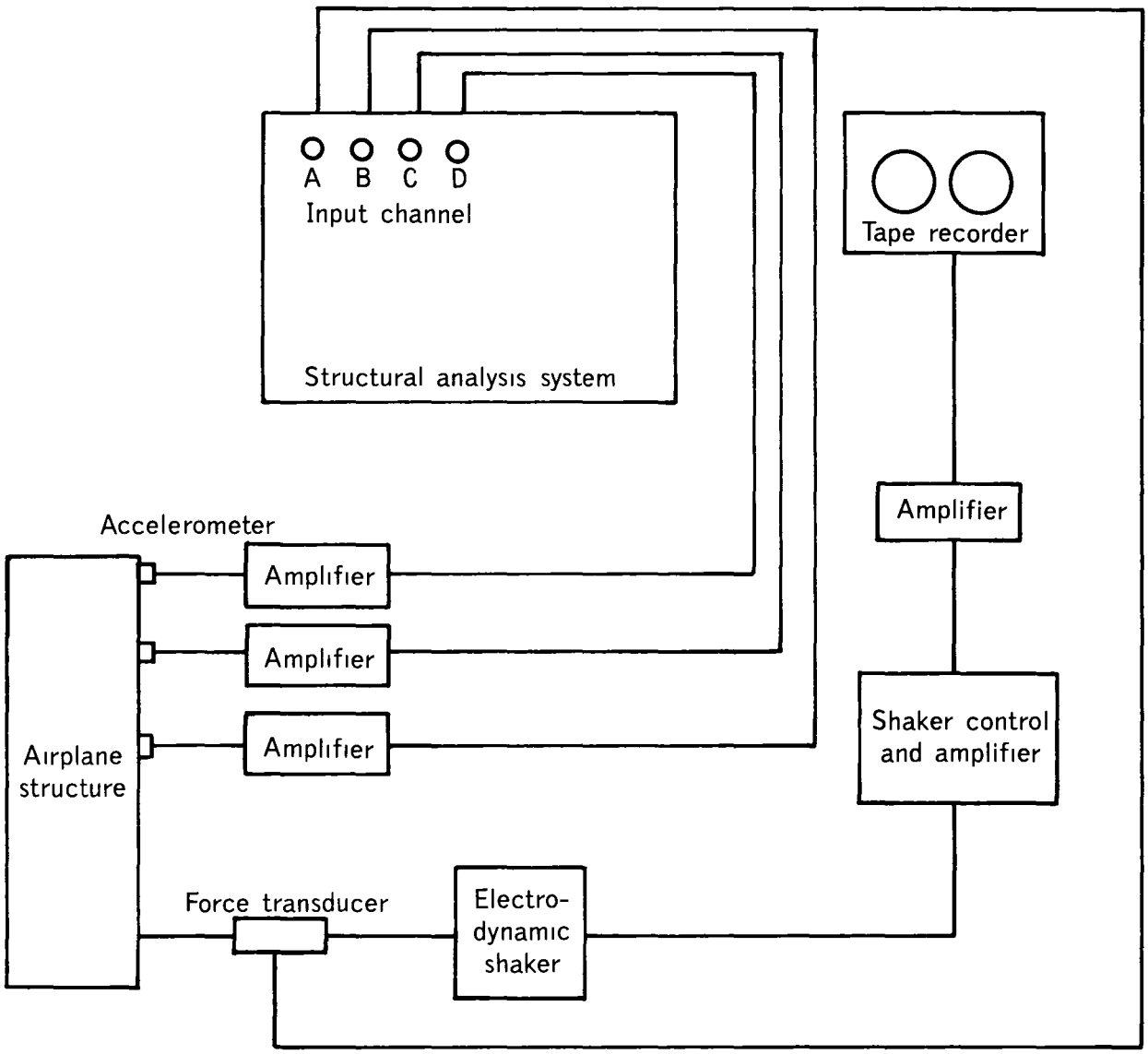

Figure 15 Schematic of the minicomputer-based structural analysis system for random excitation

Appendix A

Frequency Sweep Data

This appendix contains the frequency sweep data obtained during the ground vibration test Noted on each plot are the shaker location, shaker force level, frequency range, and accelerometer location The accelerometer locations are shown in figure 10 Table A1 summarizes all the frequency sweeps

The frequency sweeps are contained in figures A1 through A17 Figures A1 through A6 are the symmetric sweeps, and figures A7 through A12 are the antisymmetric sweeps Figures A13 through A17 are single shaker sweeps Sweeps A1–A3 and A7–A9 were conducted to examine overall vehicle response Sweeps A4–A6 and A10–A12 were conducted to better define the wing torsion motion Finally, sweeps A13–A17 were performed to define control surface modes

TABLE A1 FREQUENCY SWEEP SUMMARY

Figure	Shaker location	Excitation	Force, lbf (rms)	Response location[a] [b]
A1	Wingtip rear spar	Symmetric	16	1,11,47
A2	Wingtip rear spar	Symmetric	16	27,29,31
A3	Wingtip rear spar	Symmetric	16	26F&A,75,75L,91
A4	Wingtip rear spar	Symmetric	38	4,20,14A
A5	Wingtip rear spar	Symmetric	38	1,5,14A
A6	Midspan rear spar	Symmetric	38	1,4,14,37,40,50
A7	Wingtip rear spar	Antisymmetric	16	1,11,47
A8	Wingtip rear spar	Antisymmetric	16	27,29,31
A9	Wingtip rear spar	Antisymmetric	16	26F&A,75,75L,91
A10	Wingtip rear spar	Antisymmetric	38	4,20,14A
A11	Wingtip front spar	Antisymmetric	38	1,5,14A
A12	Midspan rear spar	Antisymmetric	38	1,4,14,37,40,50
A13	Left aileron	Single shaker	7,14,28	11,20[c]
A14	Left aileron	Single shaker	7,14,28	11,20[d]
A15	Left outboard flap	Single shaker	7,10,14	14A,22
A16	Left inboard flap	Single shaker	7,14,20	24,16
A17	Krueger flap	Single shaker	5,10	43,43A

[a] See figure 10 for response locations
[b] All directions vertical except L = Lateral and F&A = Fore and aft
[c] Hydraulics off
[d] Hydraulics on

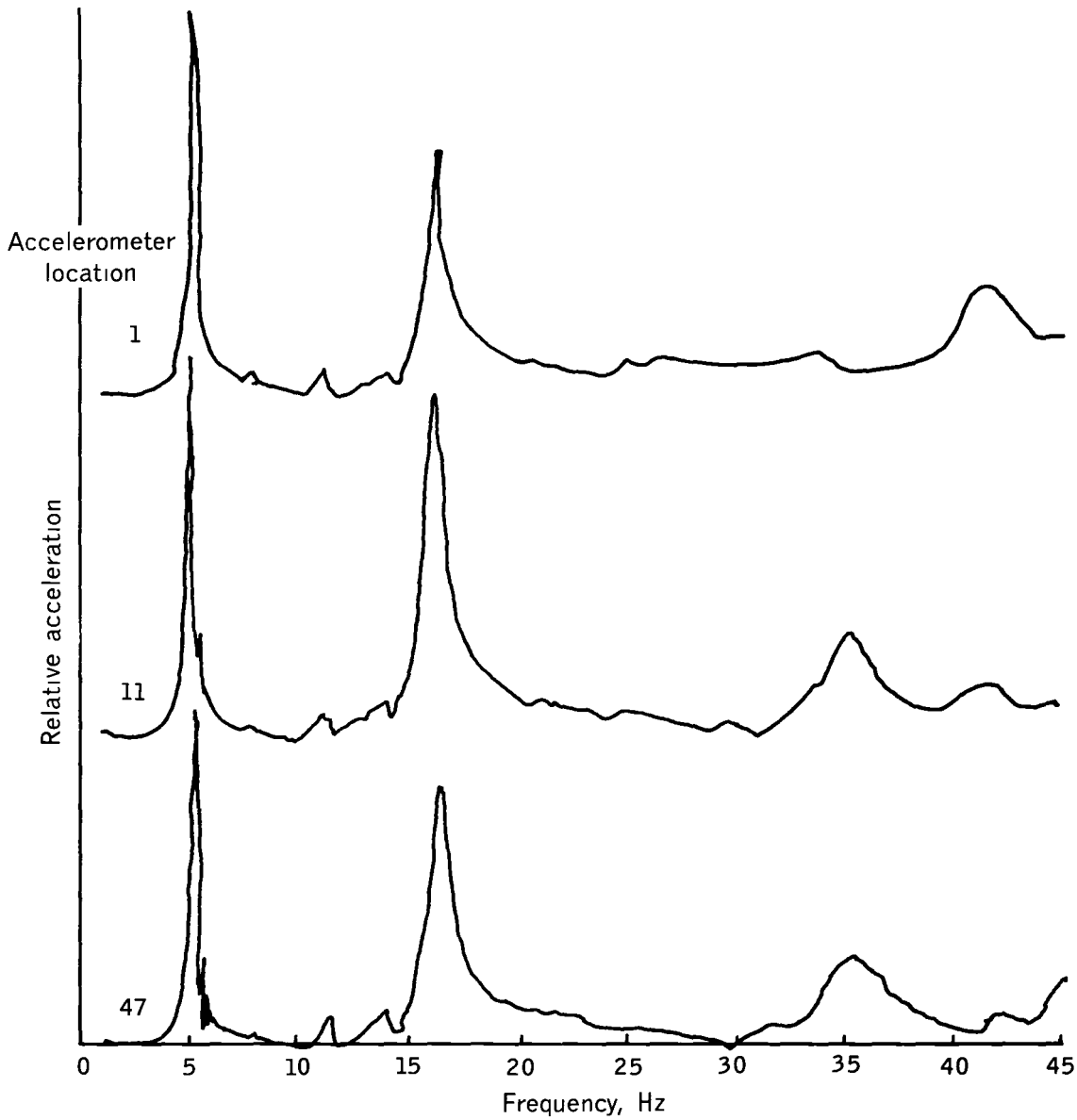

Figure A1 Frequency sweep plot for symmetric vertical excitation, wingtip rear spar shaker location, and force level of 16 lbf Accelerometer locations 1, 11, and 47

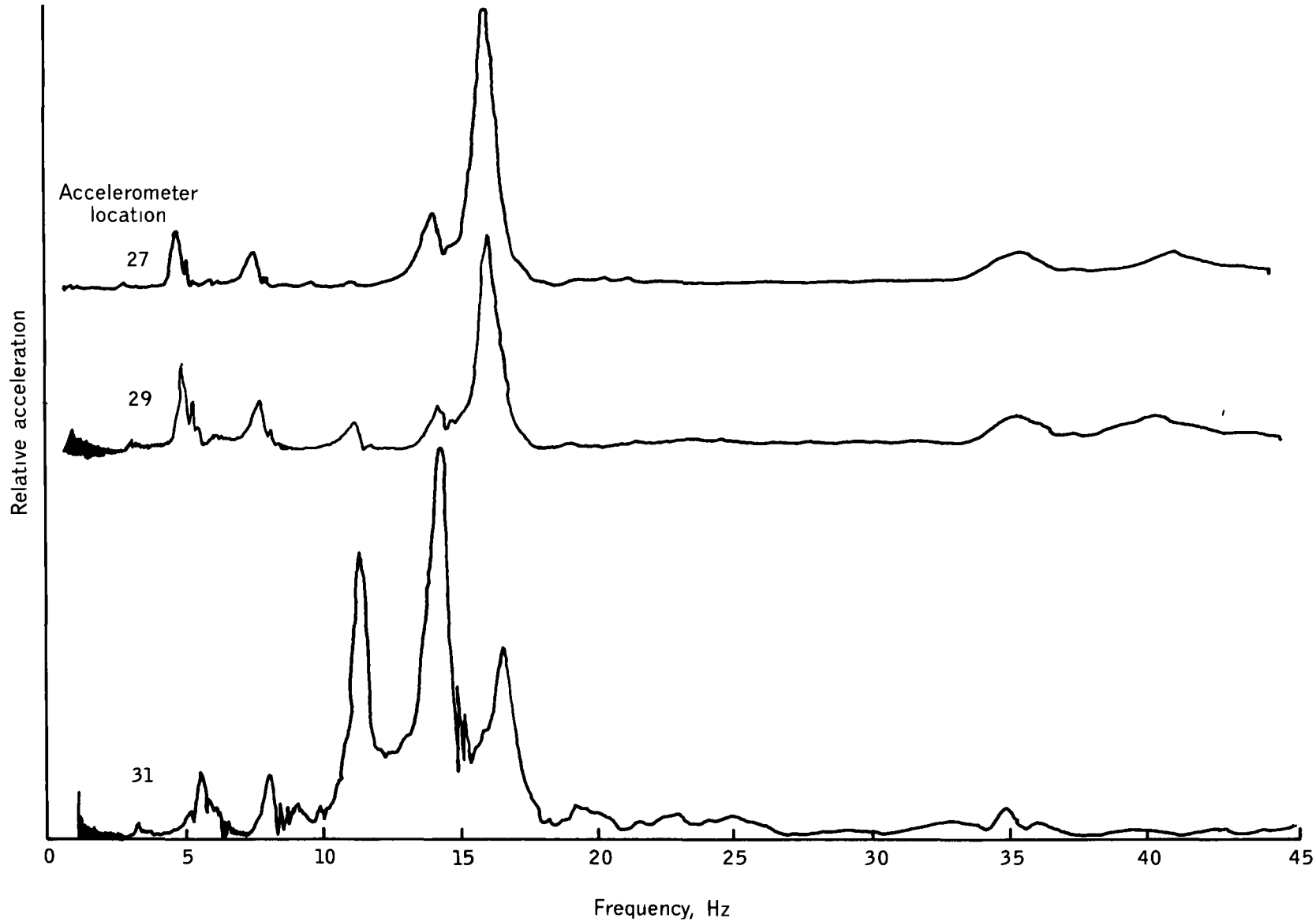

Figure A2 Frequency sweep plot for symmetric vertical excitation, wingtip rear spar shaker location, and force level of 16 lbf Accelerometer locations 27, 29, and 31

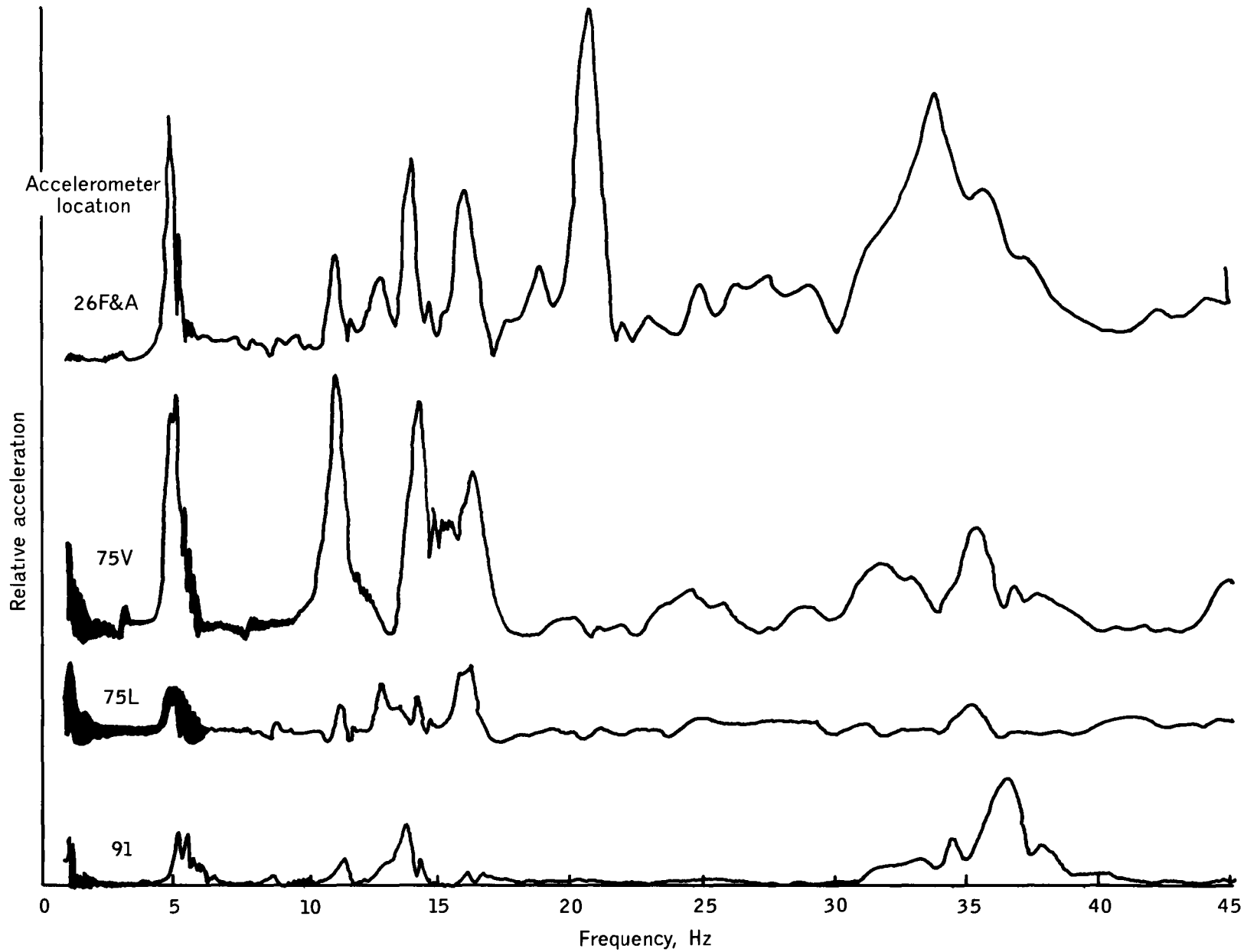

Figure A3 Frequency sweep plot for symmetric vertical excitation, wingtip rear spar shaker location, and force level of 16 lbf Accelerometer locations 26F&A, 75V, 75L, and 91

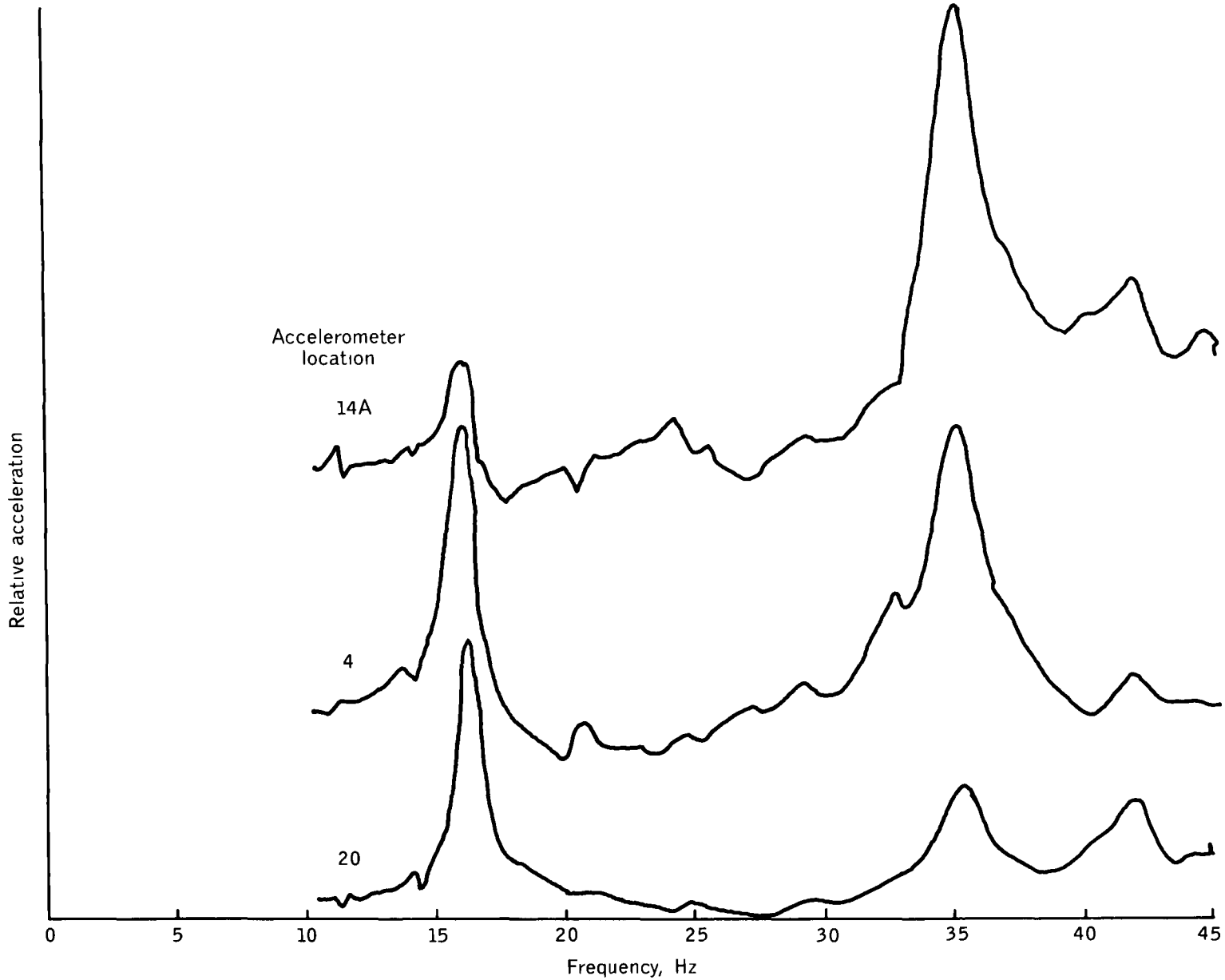

Figure A4 Frequency sweep plot for symmetric vertical excitation, wingtip rear spar shaker location, and force level of 38 lbf

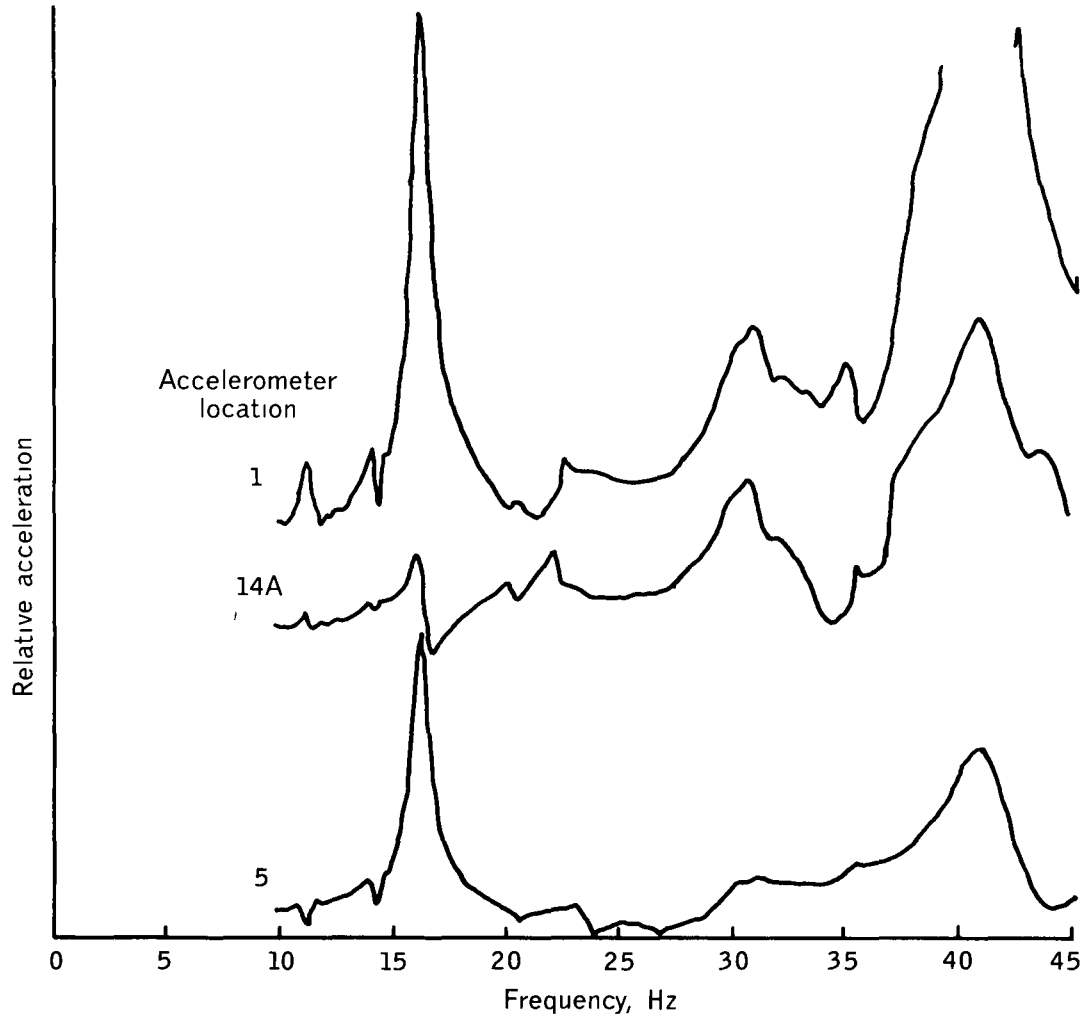

Figure A5 Frequency sweep plot for symmetric vertical excitation, wingtip front spar shaker location, and force level of 38 lbf

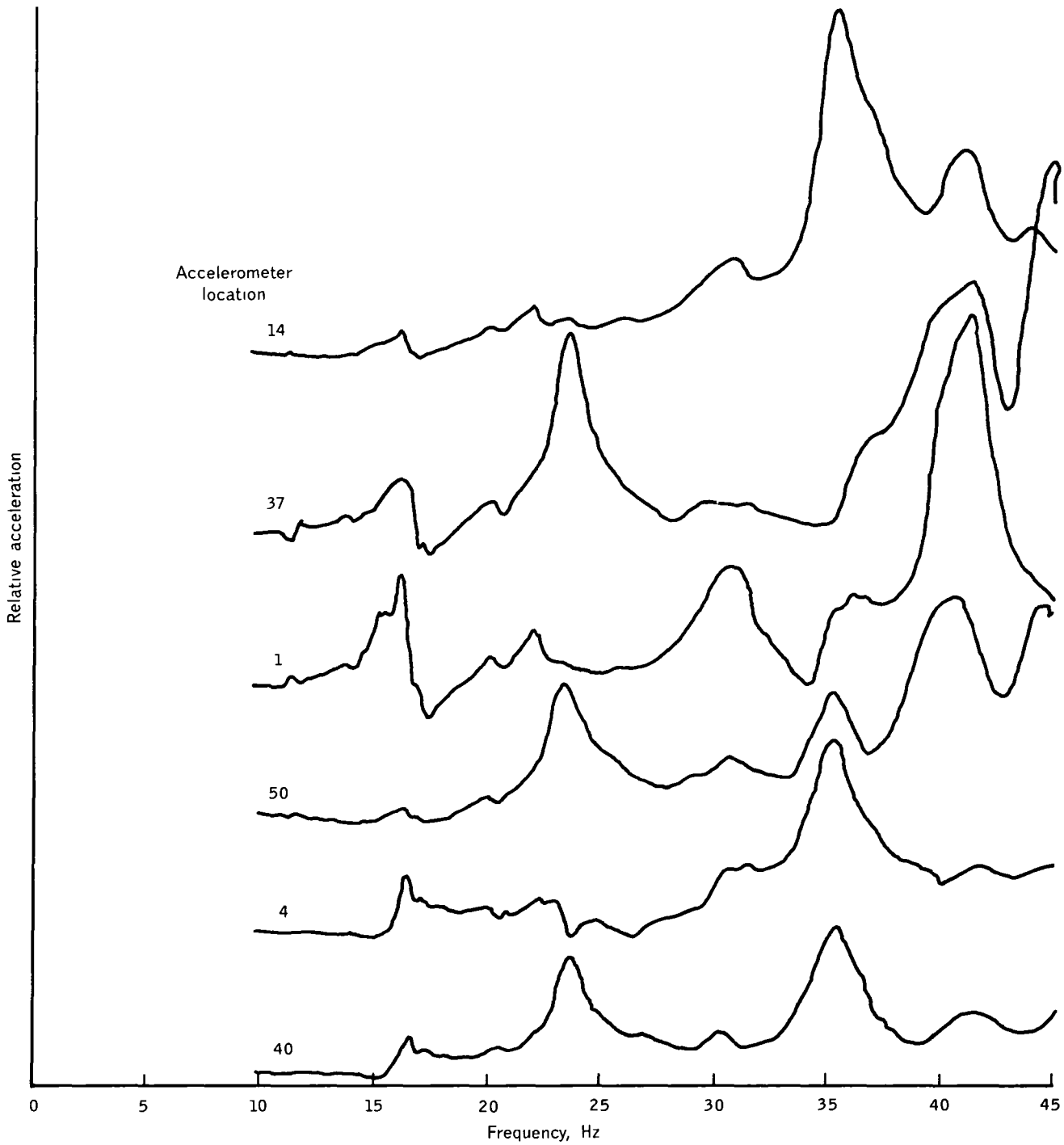

Figure A6 Frequency sweep plot for symmetric vertical excitation, midspan rear spar shaker location, and force level of 38 lbf

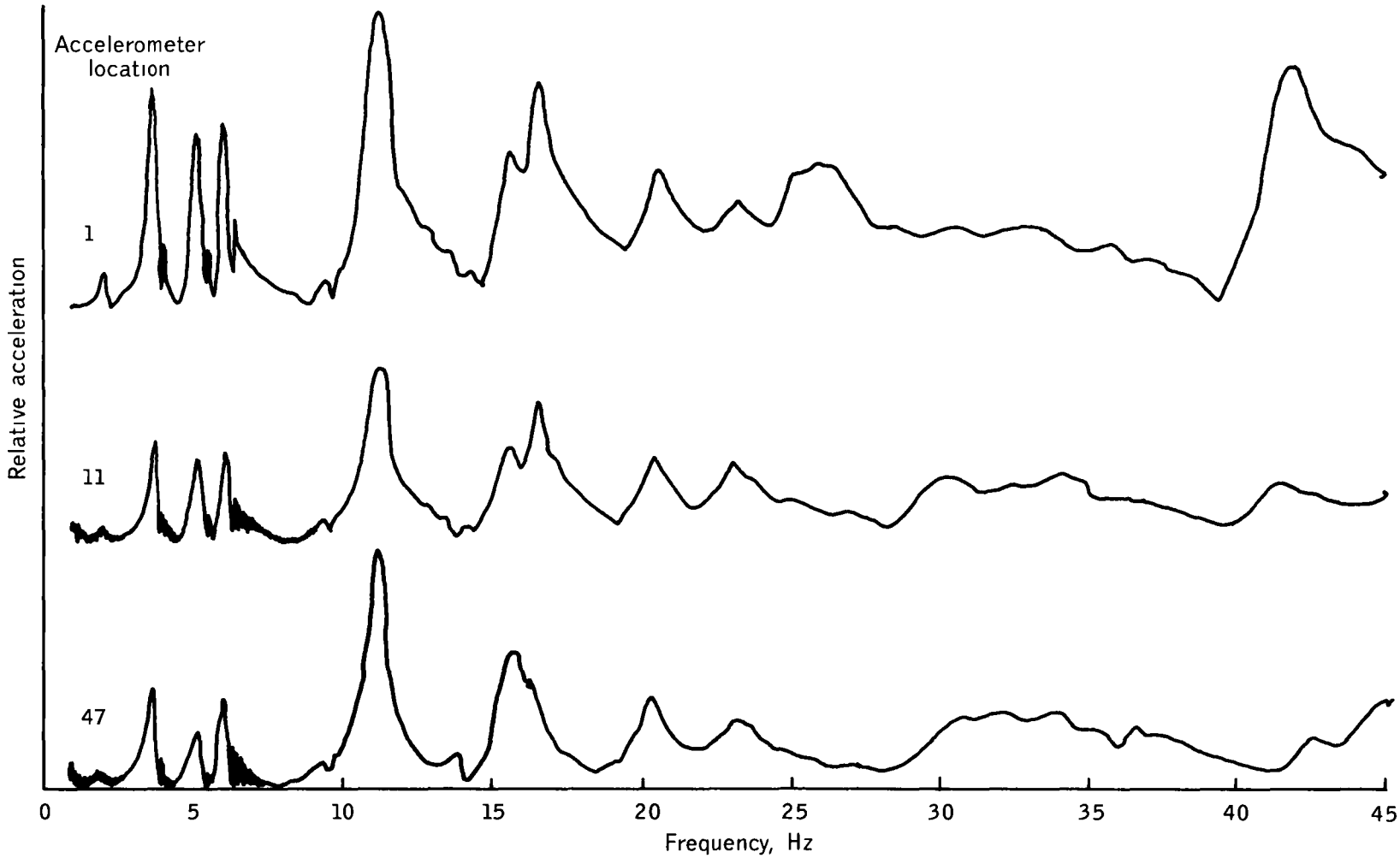

Figure A7 Frequency sweep plot for antisymmetric vertical excitation, wingtip rear spar shaker location, and force level of 16 lbf Accelerometer locations 1, 11, and 47

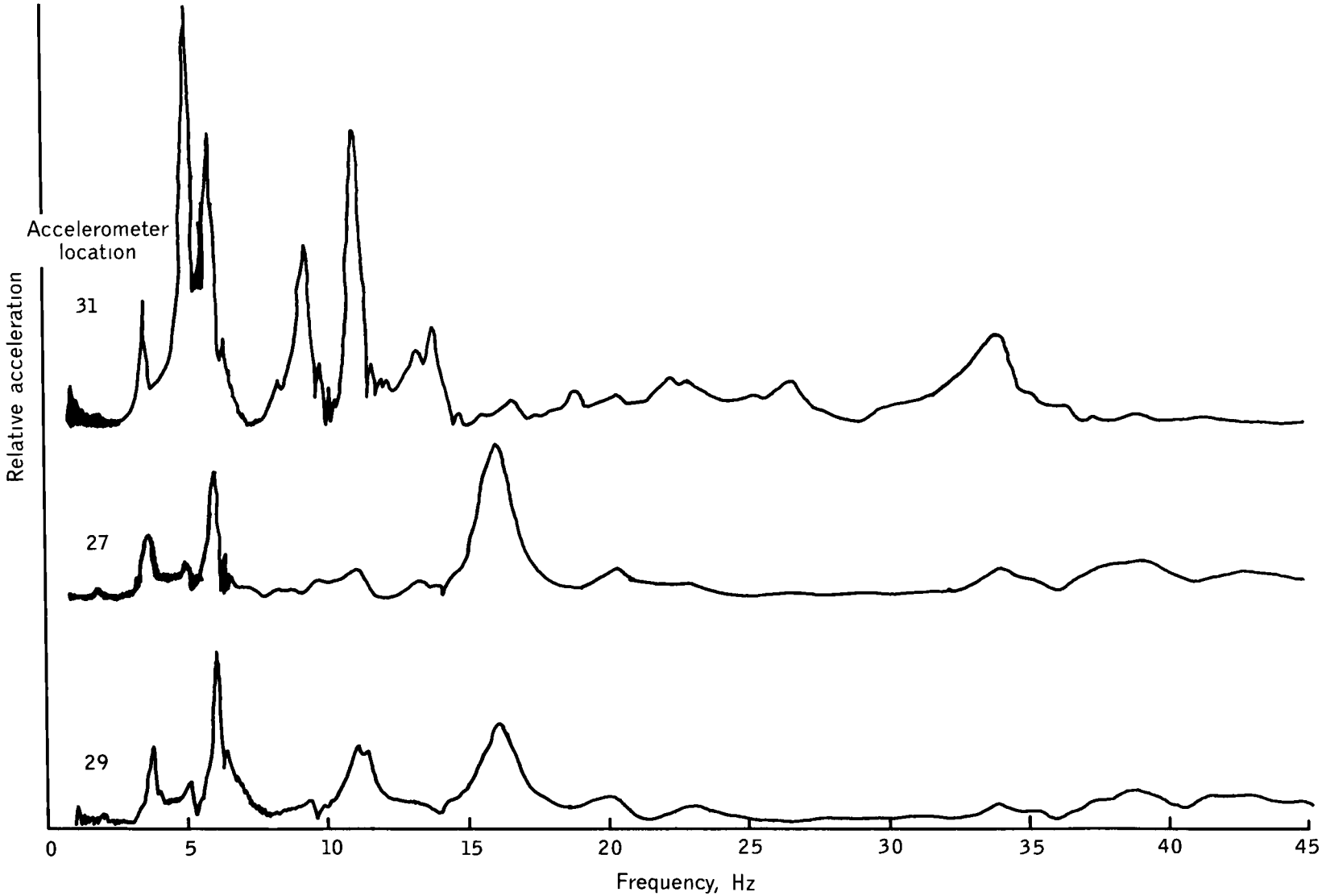

Figure A8 Frequency sweep plot for antisymmetric vertical excitation, wingtip rear spar shaker location, and force level of 16 lbf Accelerometer locations 27, 29, and 31

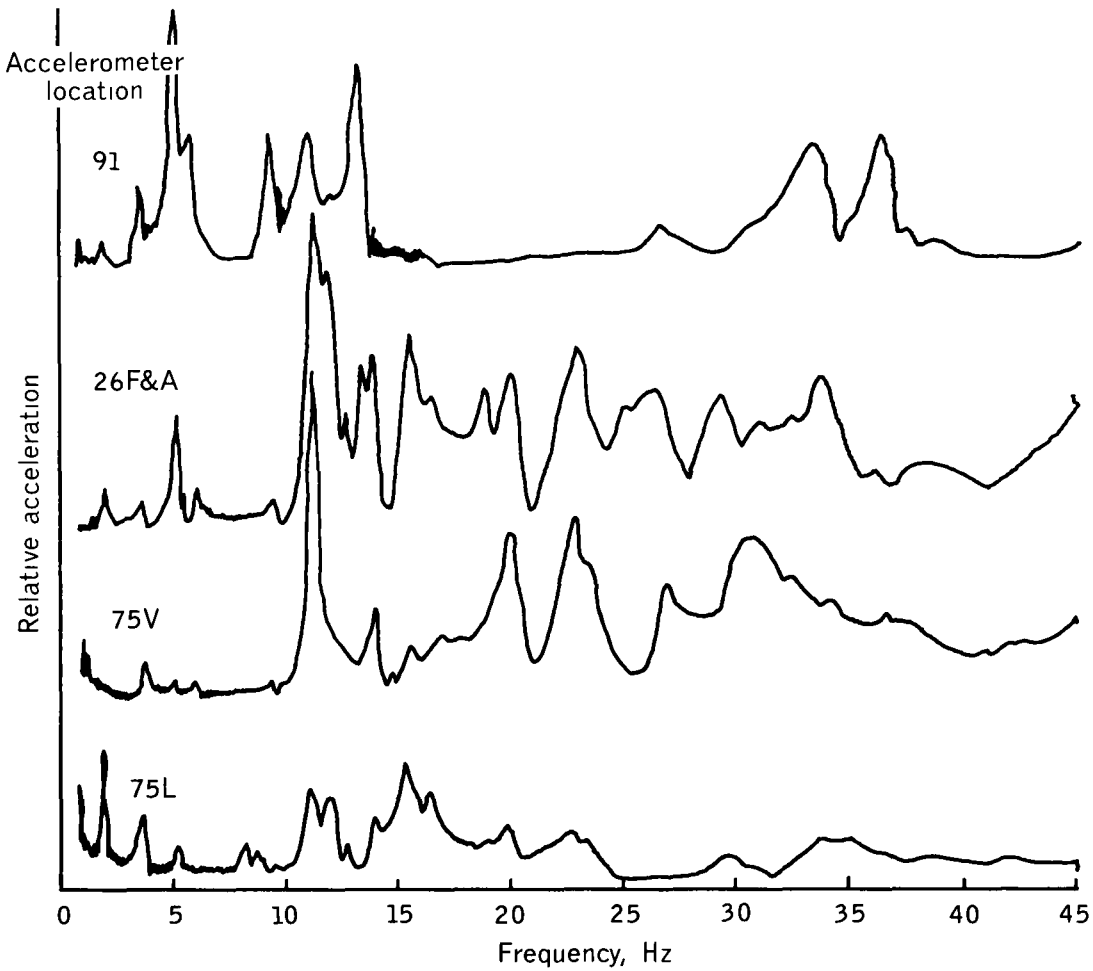

Figure A9 Frequency sweep plot for antisymmetric vertical excitation, wingtip rear spar shaker location, and force level of 16 lbf Accelerometer locations 91, 26F&A, 75V, 75L, and 91

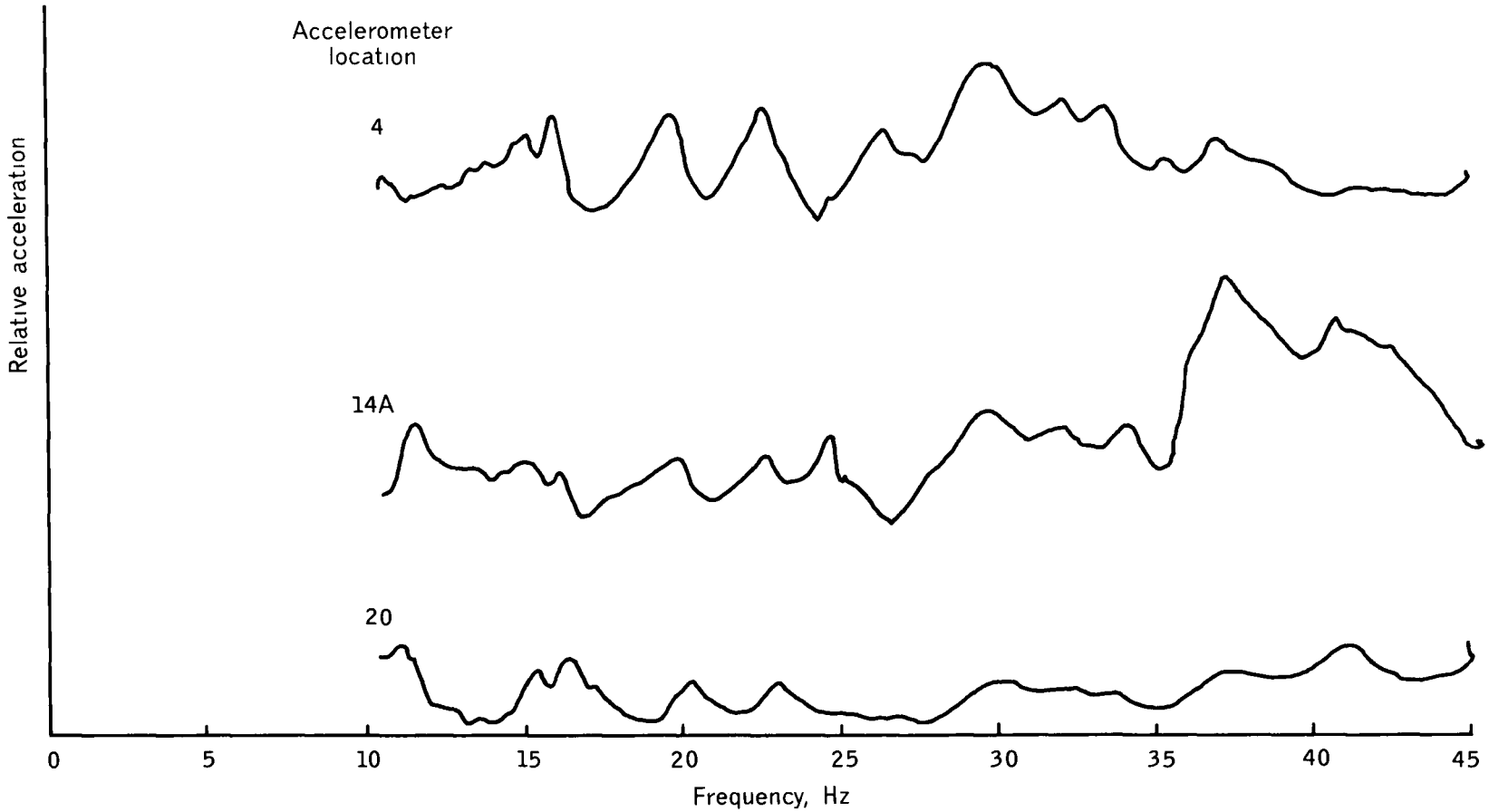

Figure A10 Frequency sweep plot for antisymmetric vertical excitation, wingtip rear spar shaker location, and force level of 38 lbf

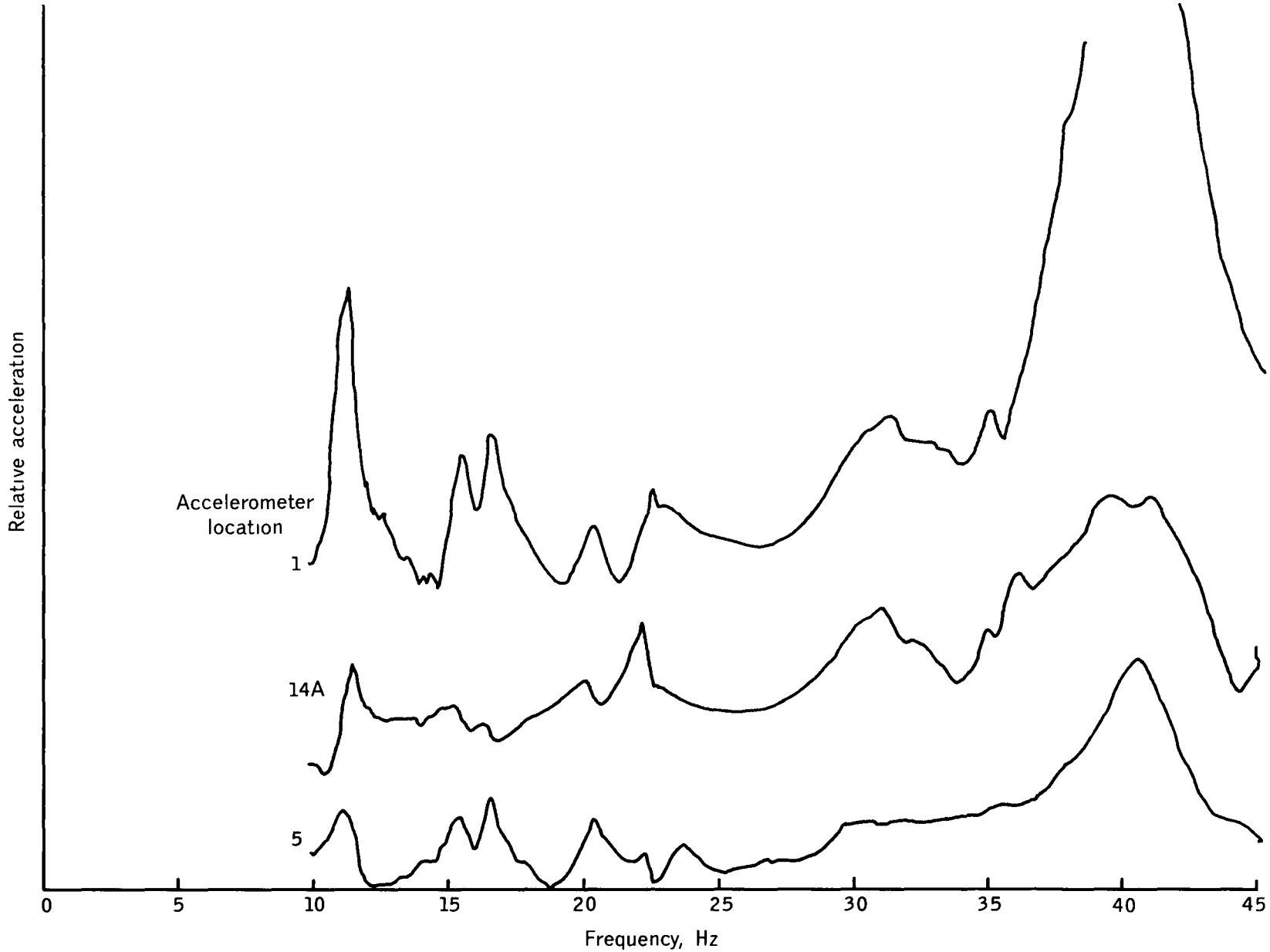

Figure A11 Frequency sweep plot for antisymmetric vertical excitation, wingtip front spar shaker location, and force level of 38 lbf

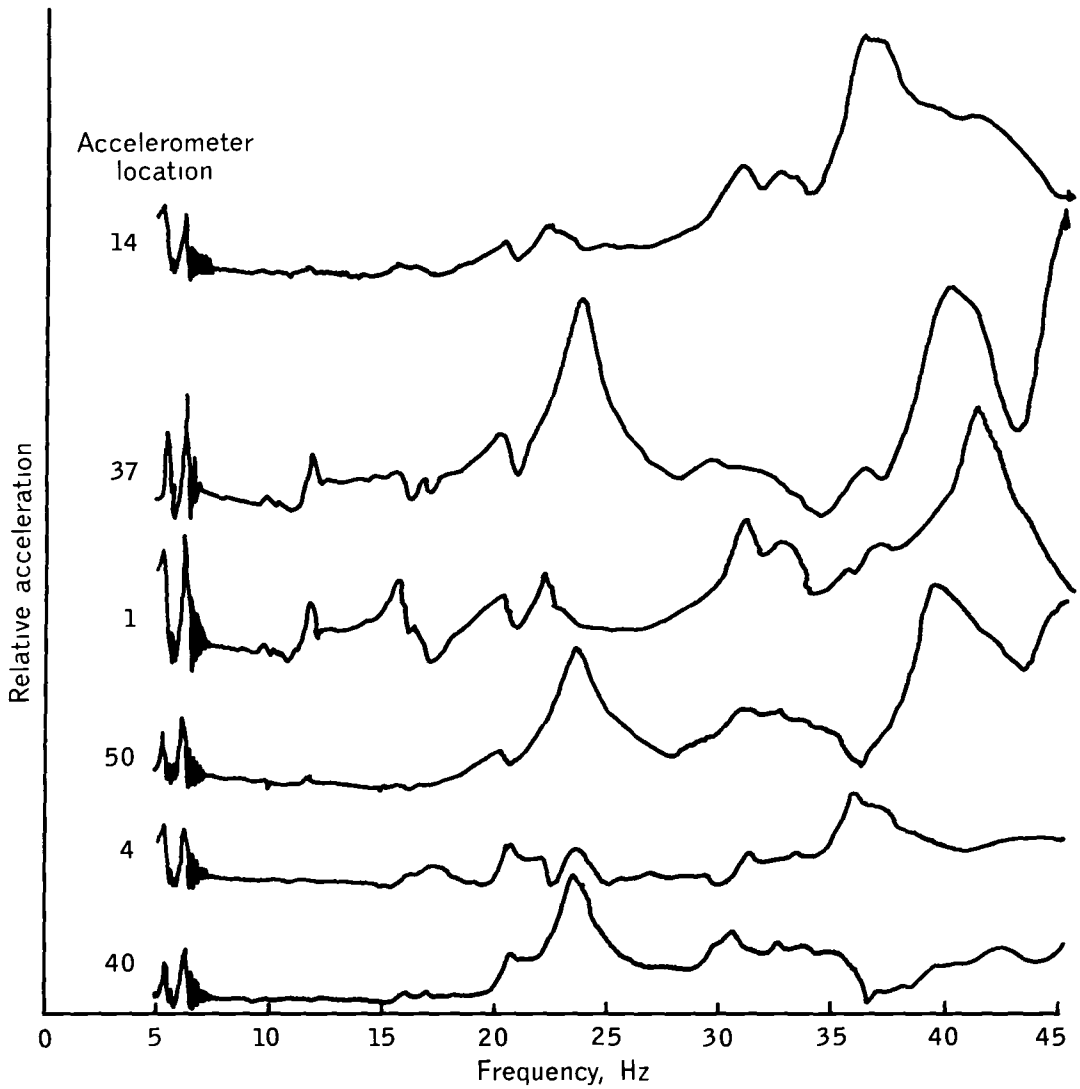

Figure A12 Frequency sweep plot for antisymmetric vertical excitation, wing midspan rear spar shaker location, and force level of 38 lbf

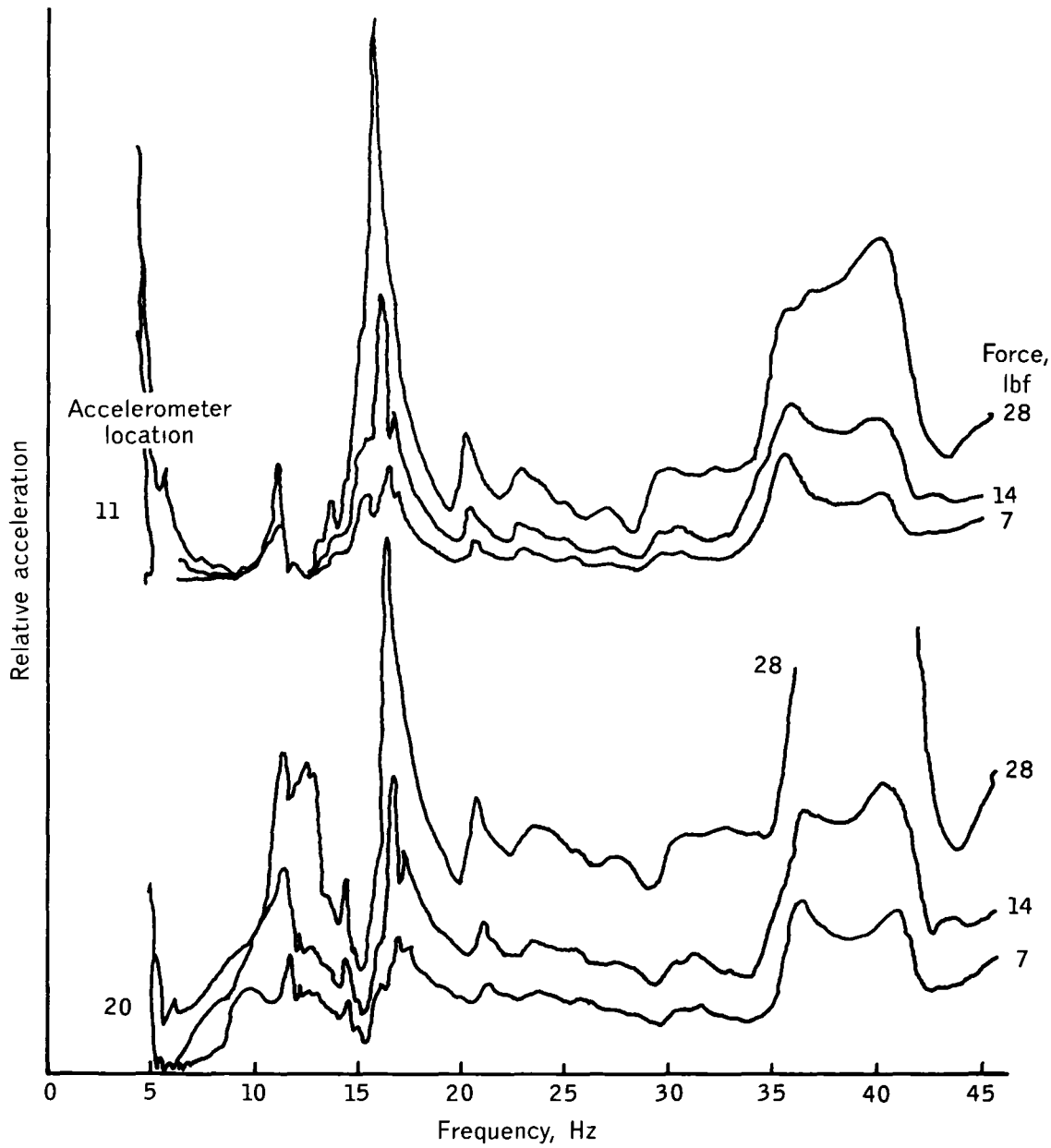

Figure A13 Frequency sweep plot for single shaker vertical excitation on left aileron with three force levels Hydraulic power off

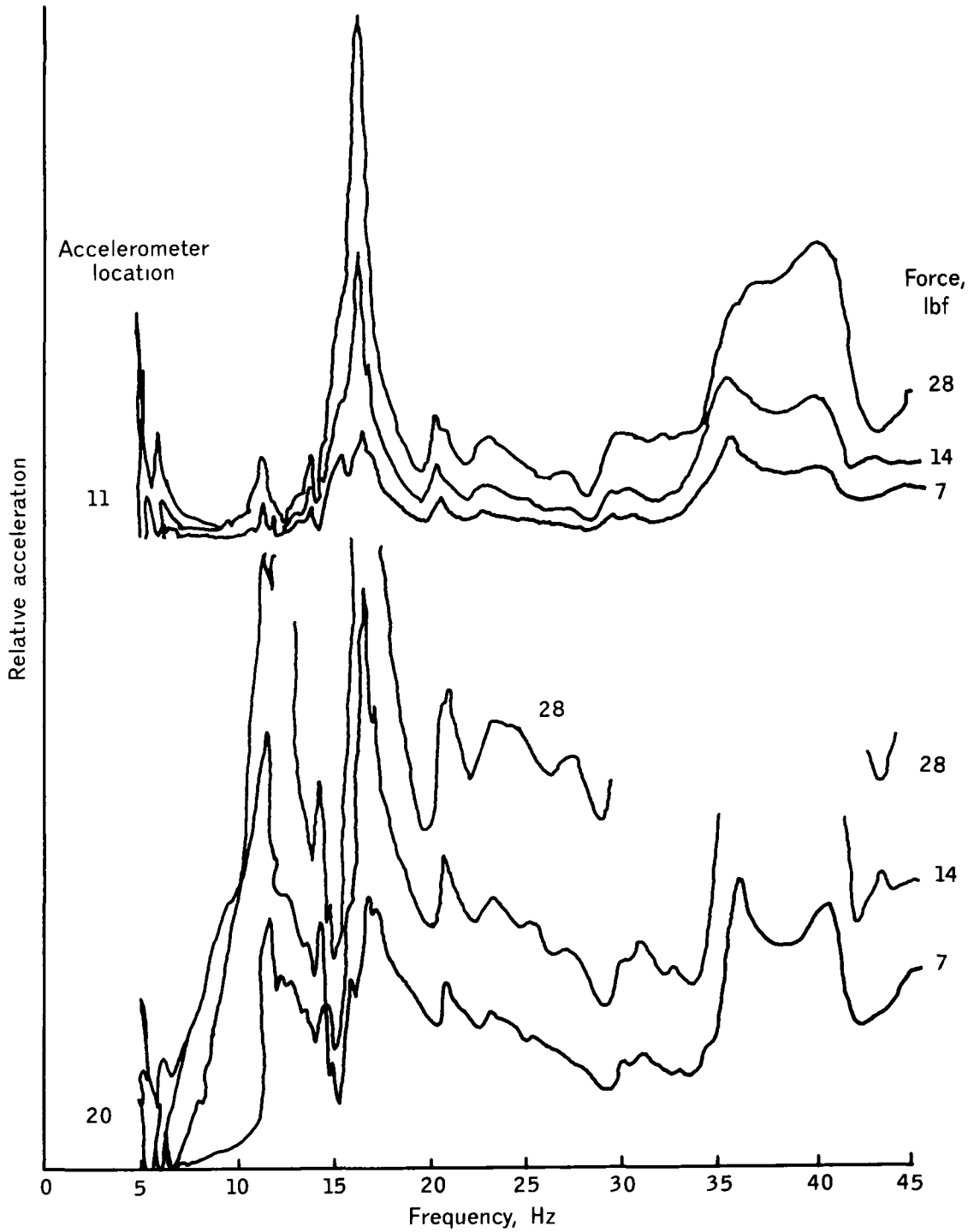

Figure A14 Frequency sweep plot for single shaker vertical excitation on left aileron with three force levels Hydraulic power on

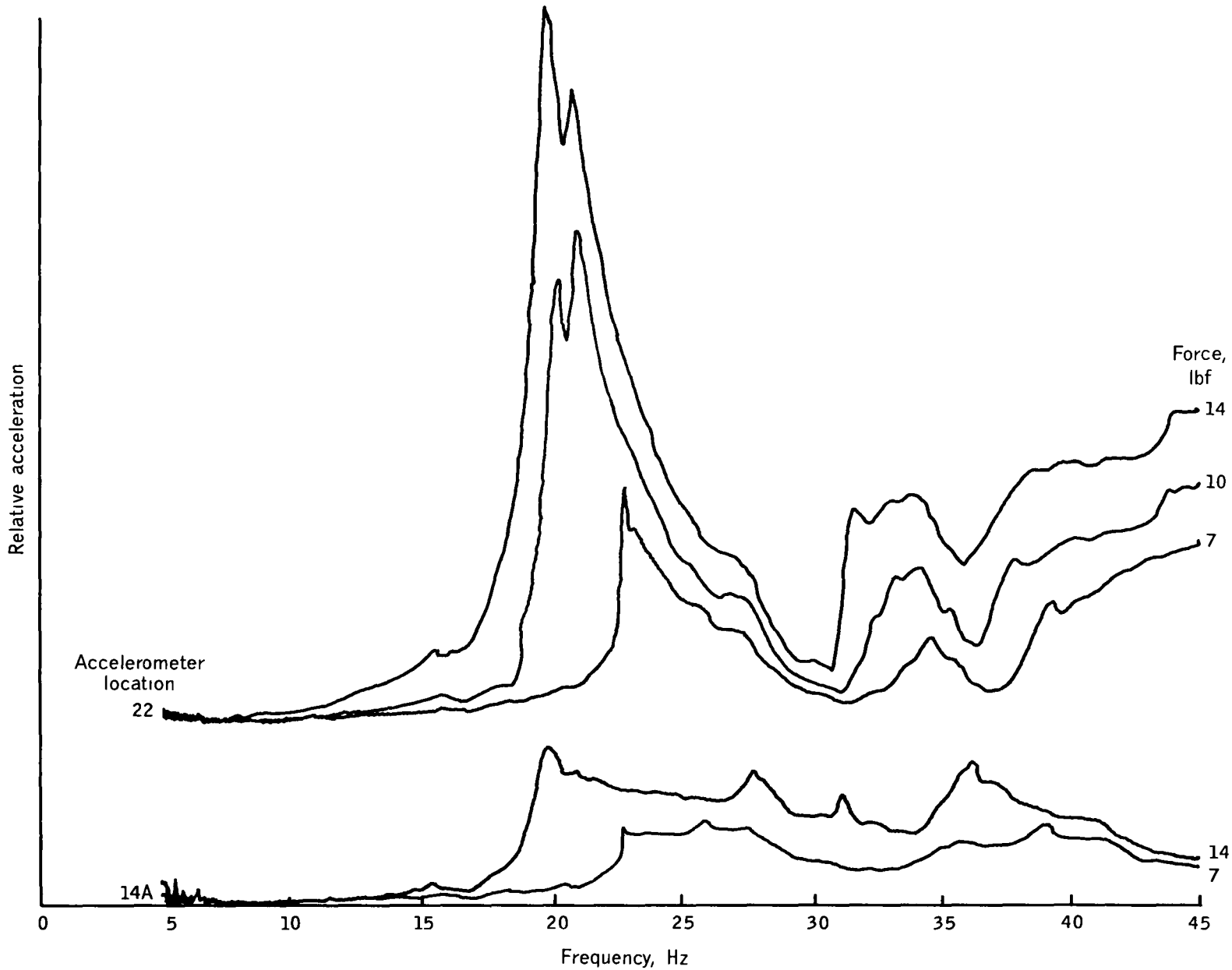

Figure A15 Frequency sweep plot for single shaker on left outboard flap for three force levels

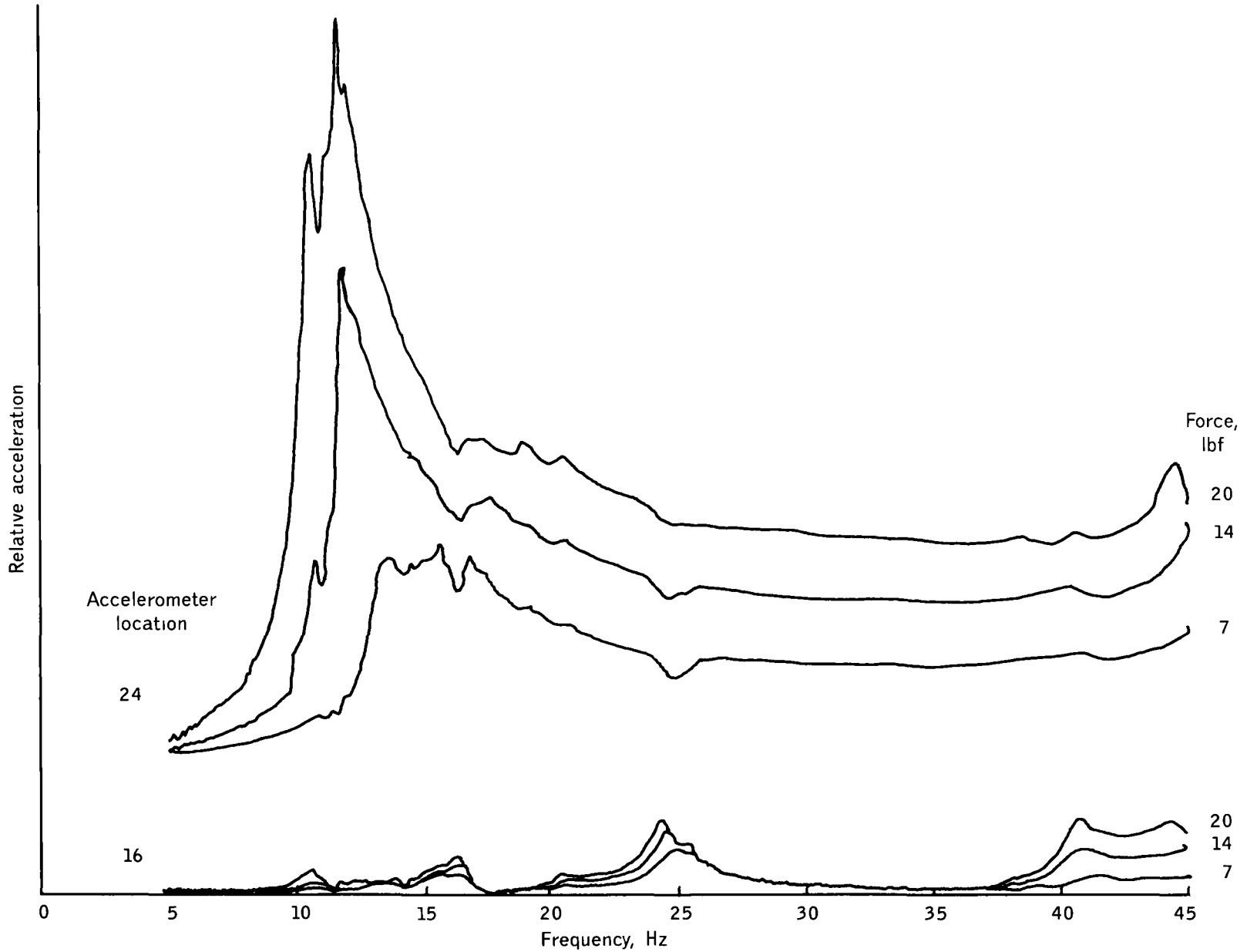

Figure A16 Frequency sweep plot for single shaker excitation on left inboard flap and three force levels

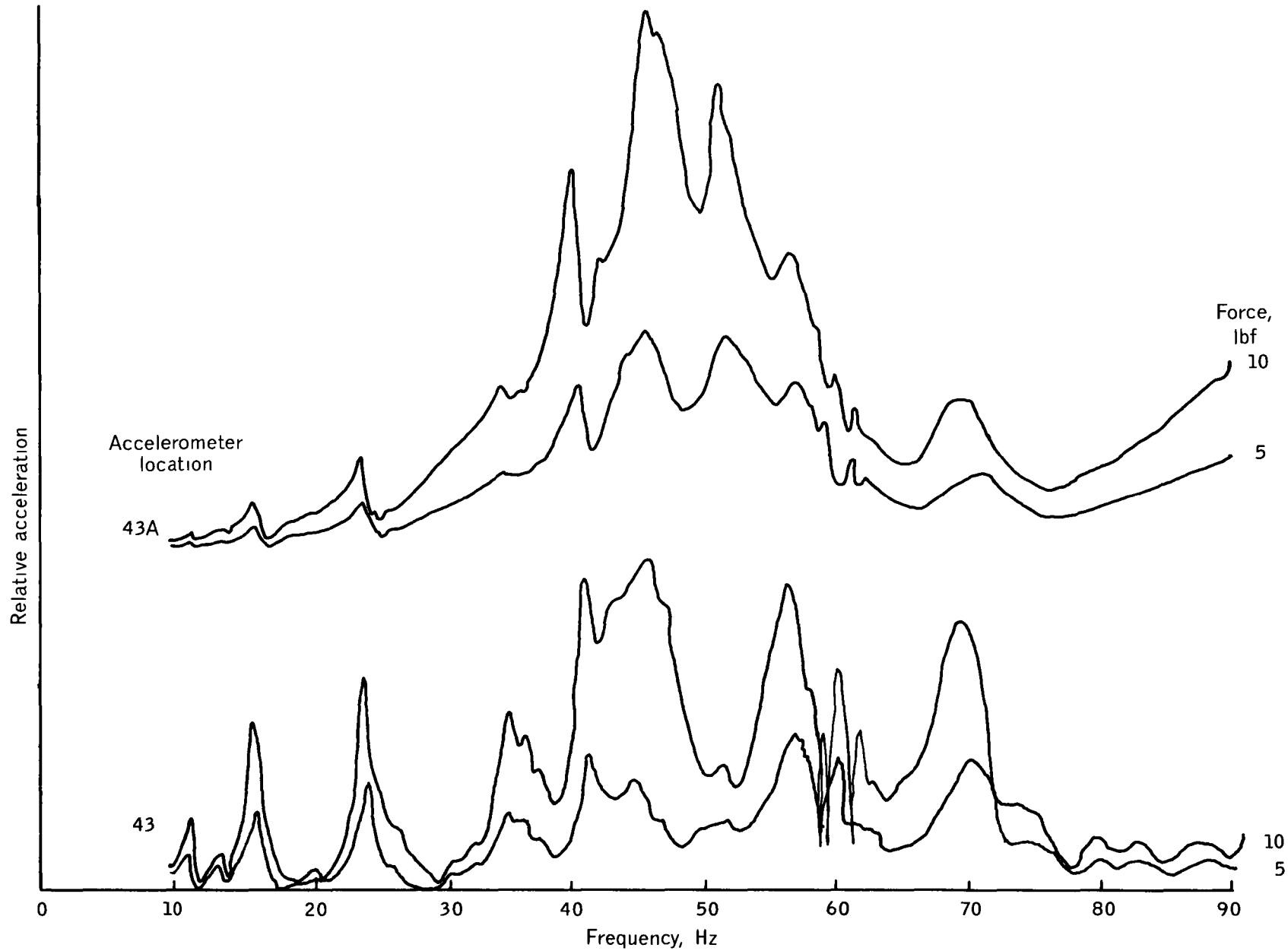

Figure A17 Frequency sweep plot for single shaker excitation on Krueger flap and two force levels

Appendix B

Random Excitation Frequency Response

Appendix B contains frequency response functions obtained from single-point-random excitation The frequency response functions are identified in table B1 and are shown in figures B1 through B20 Frequency response functions for the right and left side of the airplane are shown Each plot is identified by the location of the accelerometer used (See fig 10) The frequency scale is from 1 to 50 Hz to facilitate a comparison with the sine-dwell method All the symmetric and antisymmetric modes should be indicated by peaks in the response The vertical axis is in the units of inches per second squared (acceleration) per pound force input

TABLE B1 FREQUENCY RESPONSE FUNCTION SUMMARY

Figure	Frequency response	
	Point	Location
B1	26	Left wingtip
B2	62	Right wingtip
B3	20	Left aileron
B4	56	Right aileron
B5	22	Left outboard flap
B6	58	Right outboard flap
B7	24	Left inboard flap
B8	60	Right inboard flap
B9	27	Left outboard nacelle
B10	65	Right outboard nacelle
B11	31	Left horizontal stabilizer
B12	69	Right horizontal stabilizer
B13	35	Left elevator
B14	73	Right elevator
B15	91	Vertical fin tip
B16	92	Rudder
B17	75	Forward fuselage vertical
B18	82	Aft fuselage vertical
B19	75	Forward fuselage lateral
B20	82	Aft fuselage lateral

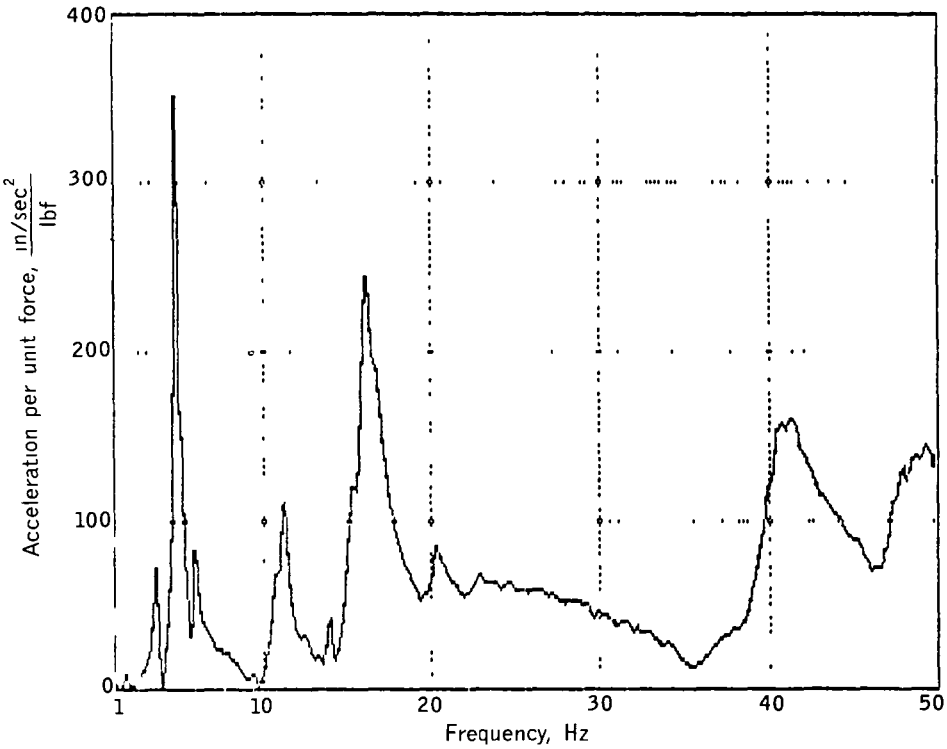

Figure B1 Left wingtip (point 26) frequency response function

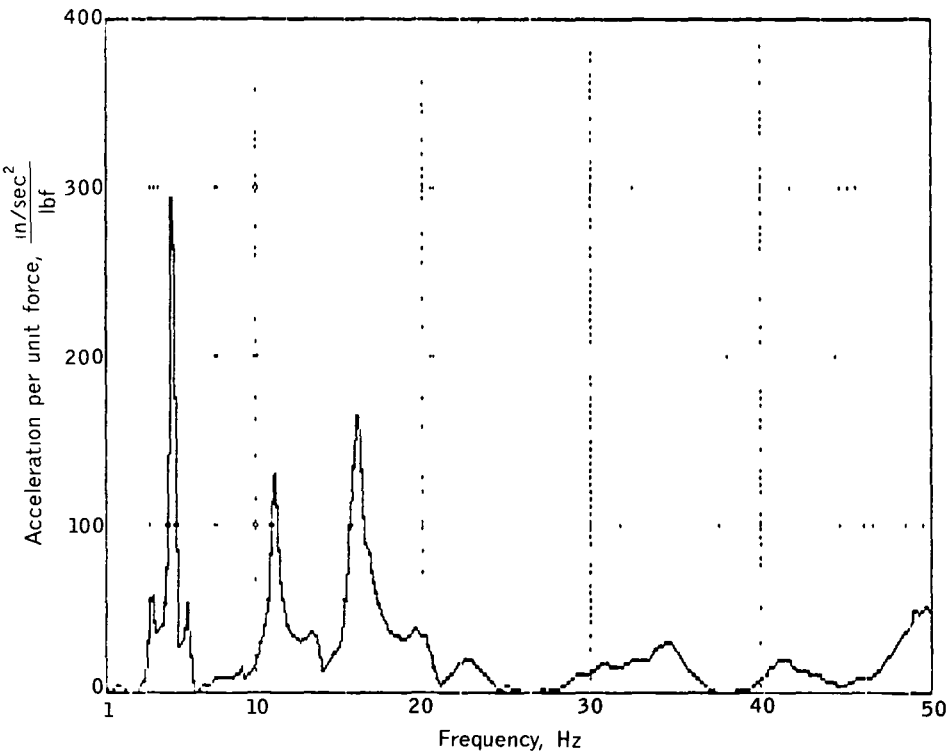

Figure B2 Right wingtip (point 62) frequency response function

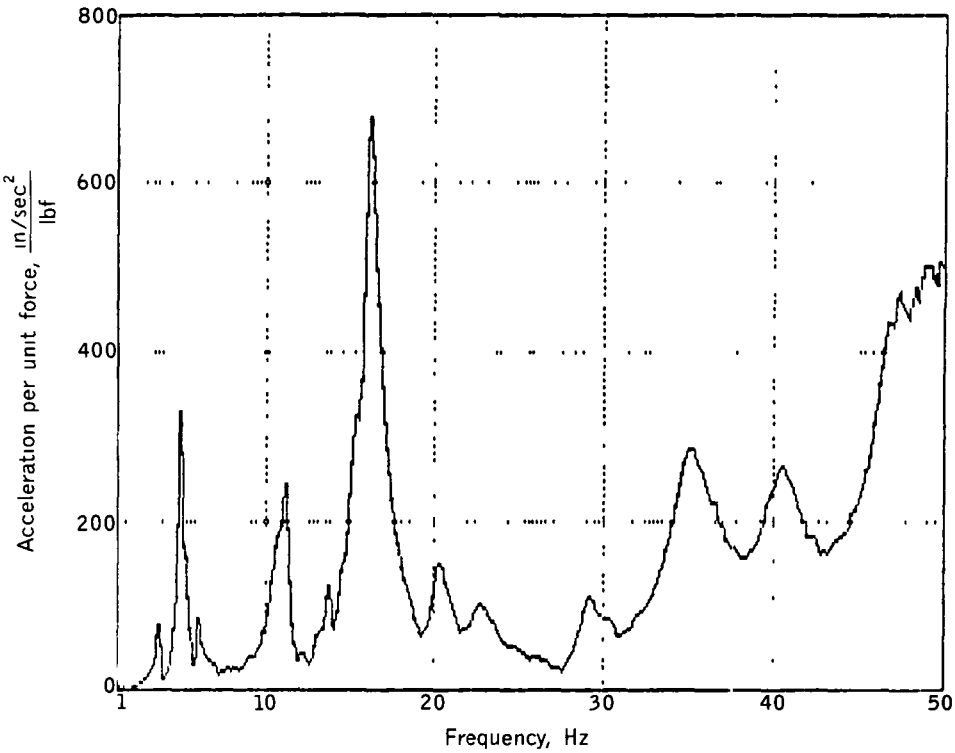

Figure B3 Left aileron (point 20) frequency response function

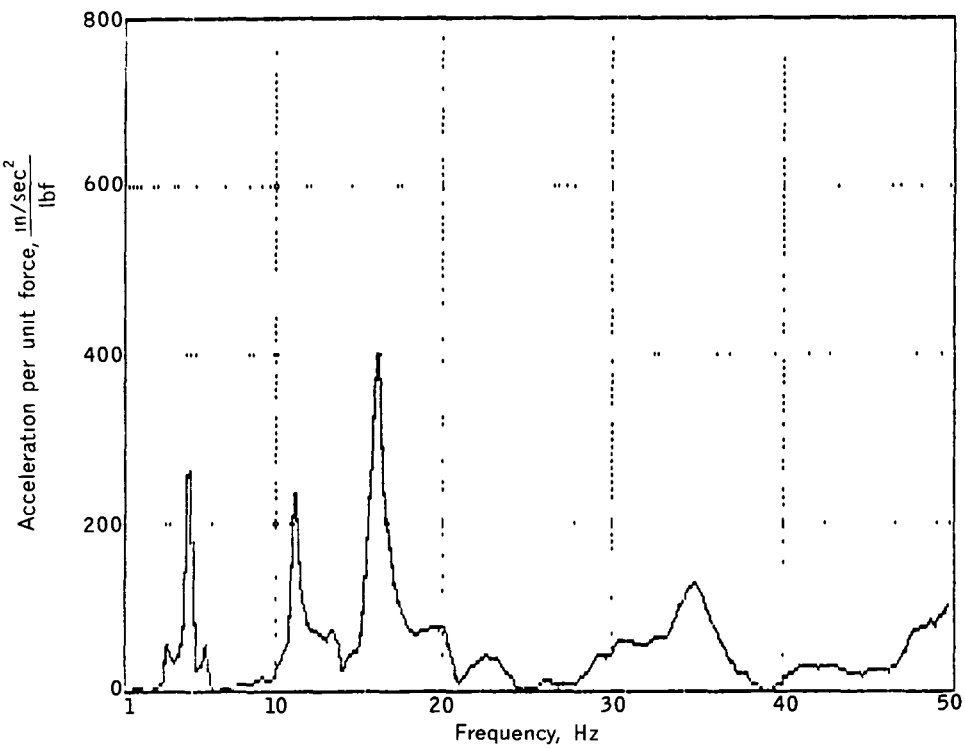

Figure B4 Right aileron (point 56) frequency response function

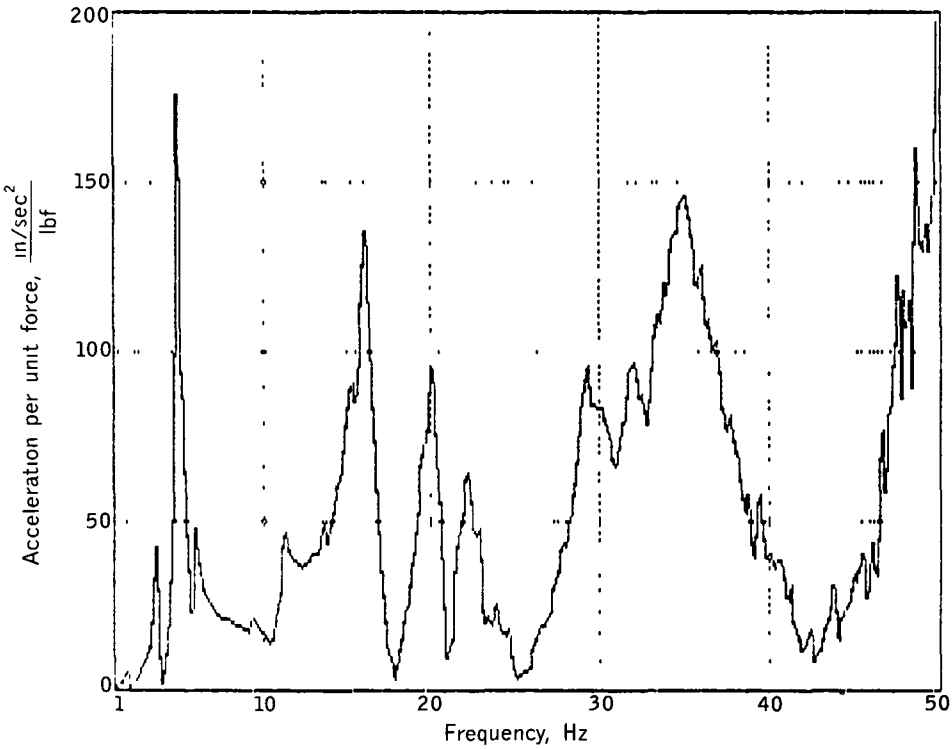

Figure B5 Left outboard trailing-edge flap (point 22) frequency response function

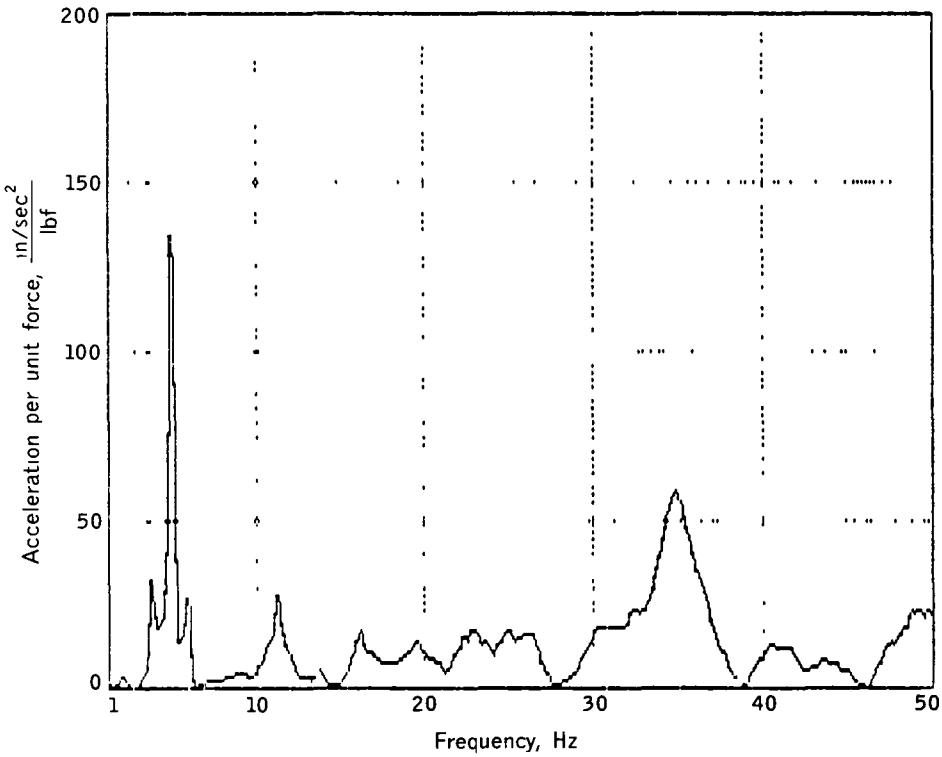

Figure B6 Right outboard trailing-edge flap (point 58) frequency response function

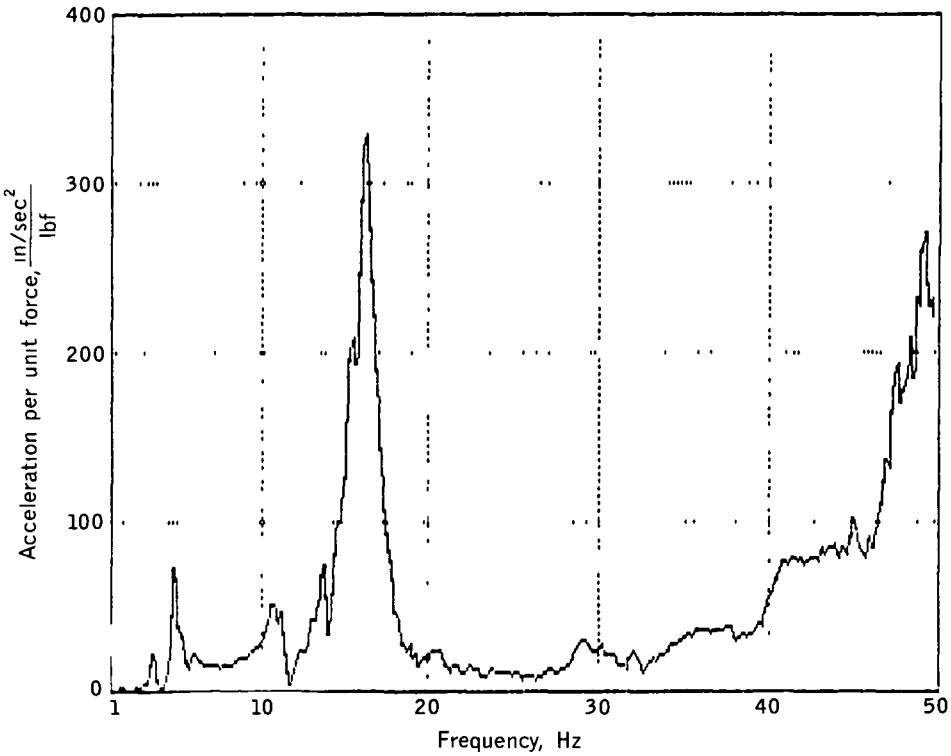

Figure B7 Left inboard trailing-edge flap (point 24) frequency response function

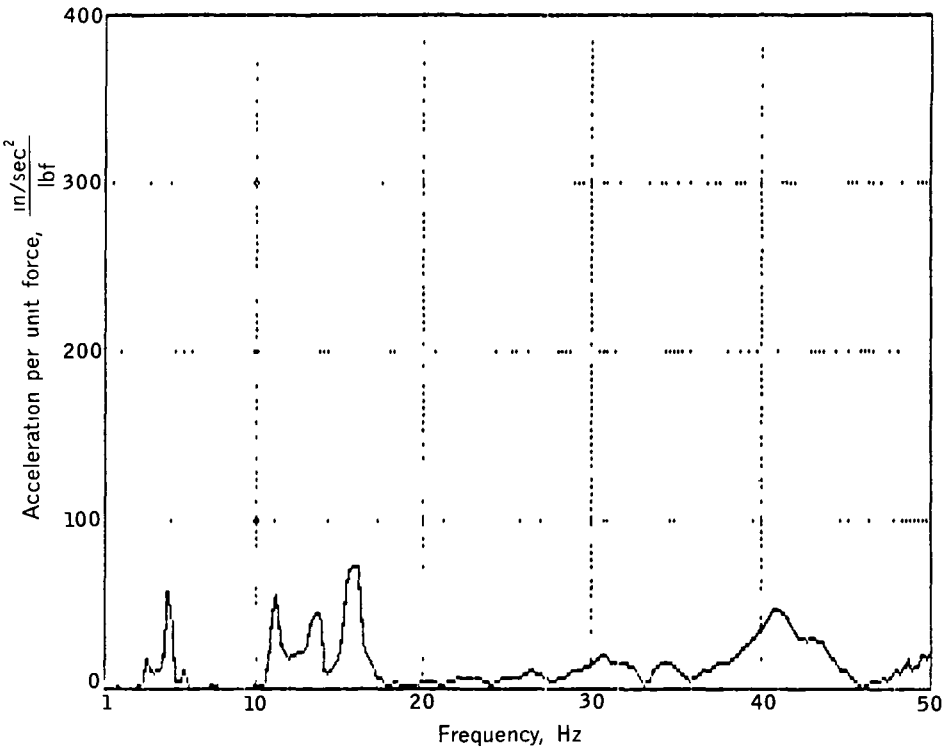

Figure B8 Right inboard trailing-edge flap (point 60) frequency response function

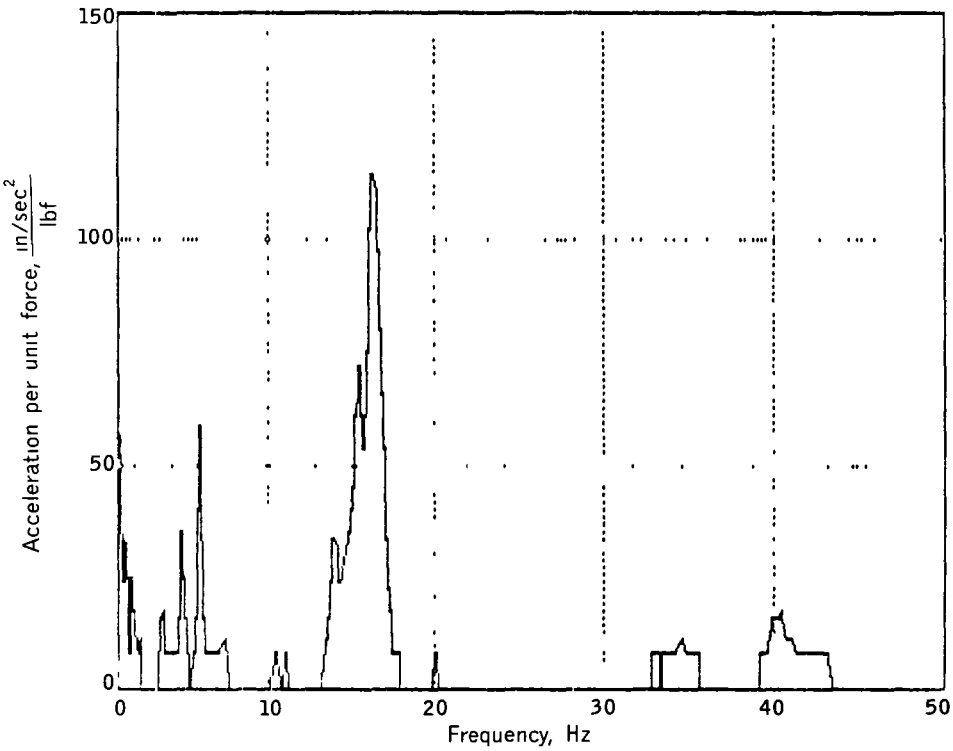

Figure B9 Left outboard engine nacelle (point 27) frequency response function

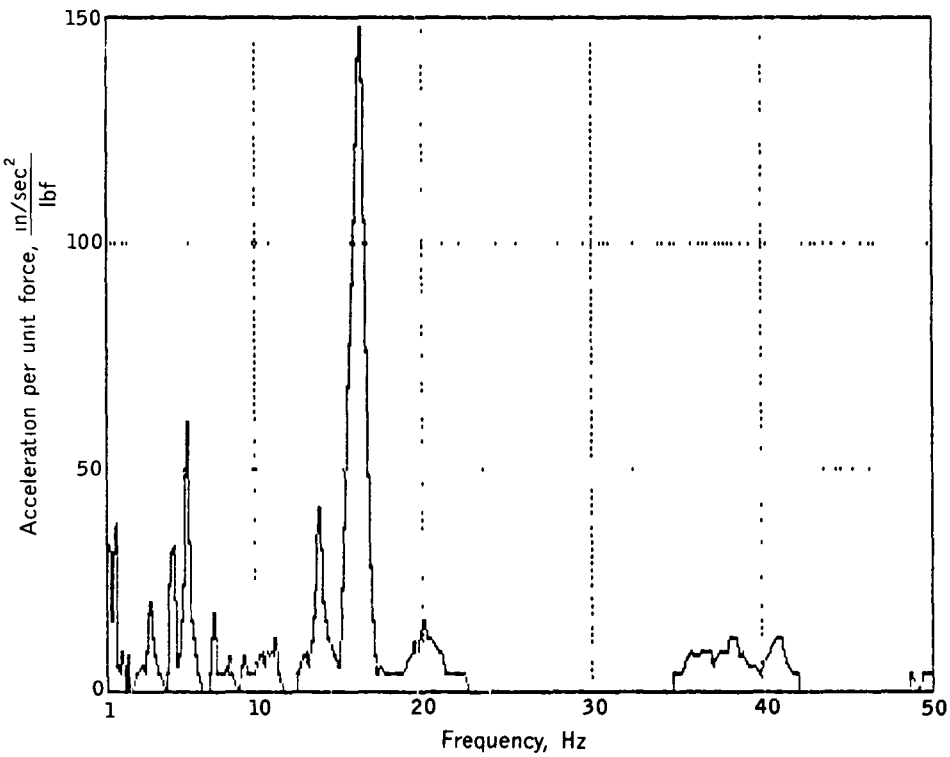

Figure B10 Right outboard engine nacelle (point 65) frequency response function

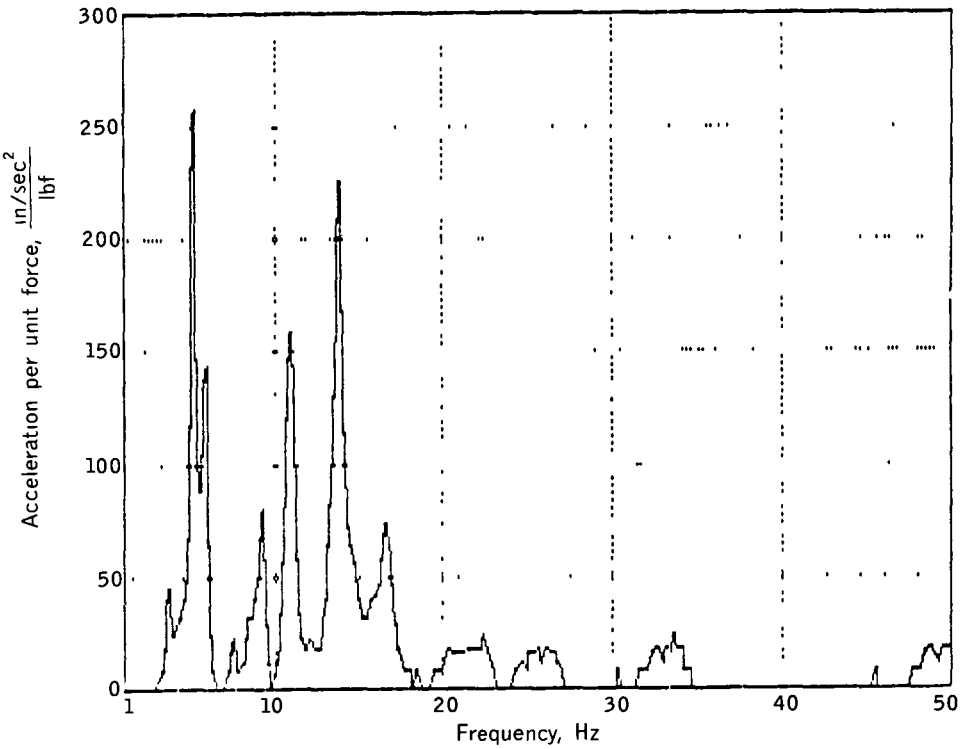

Figure B11 Left horizontal stabilizer (point 31) frequency response function

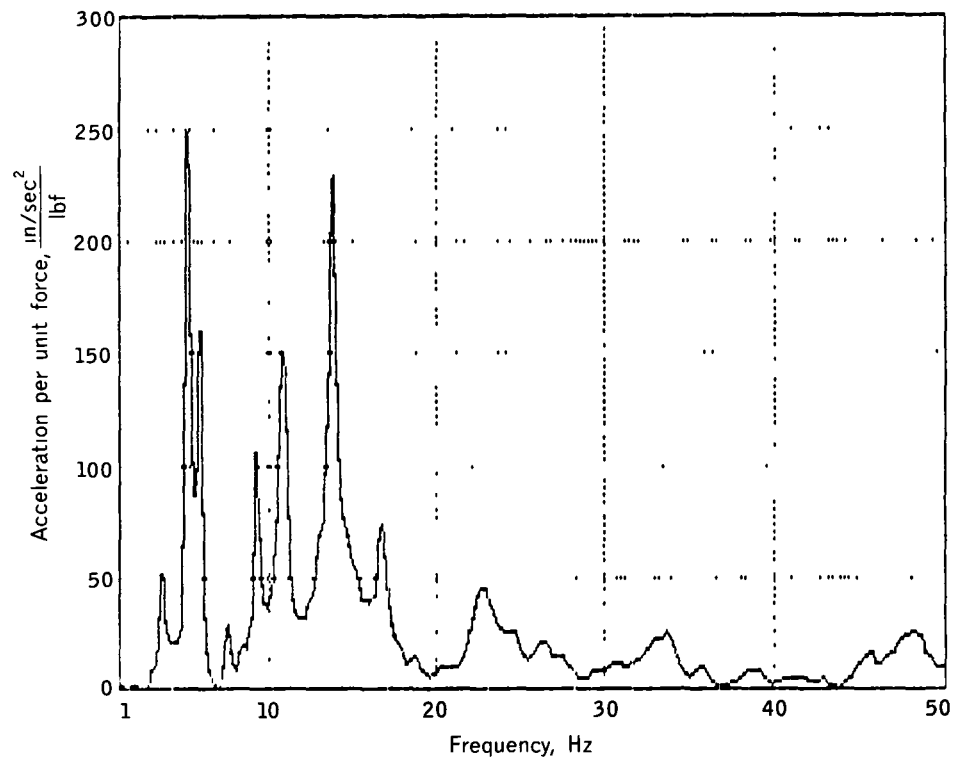

Figure B12 Right horizontal stabilizer (point 69) frequency response function

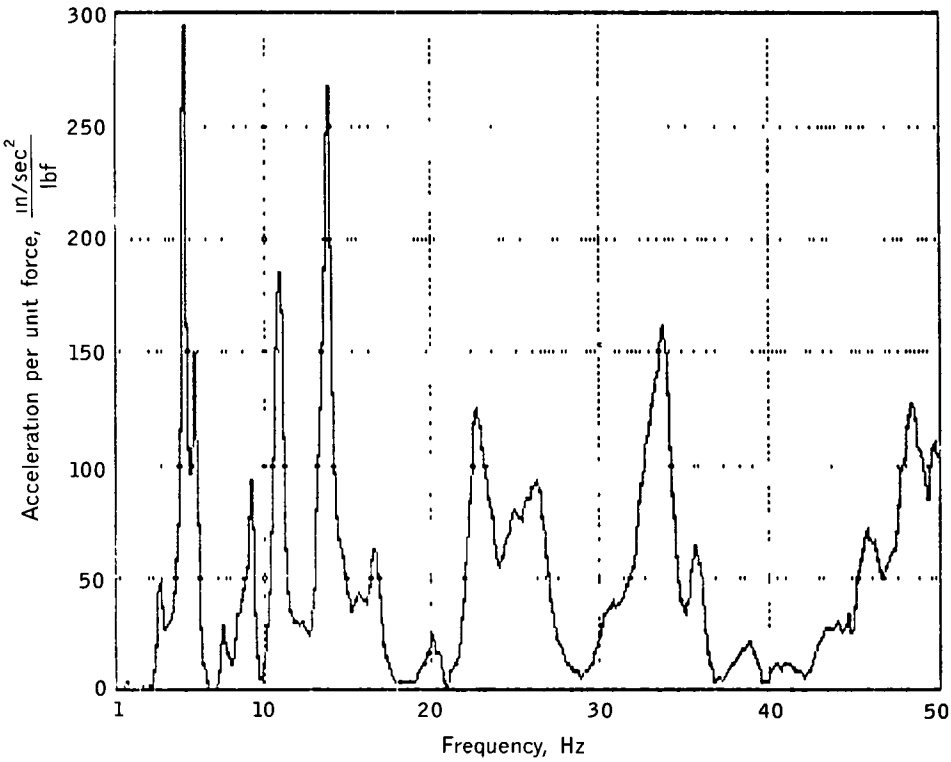

Figure B13 Left elevator (point 35) frequency response function

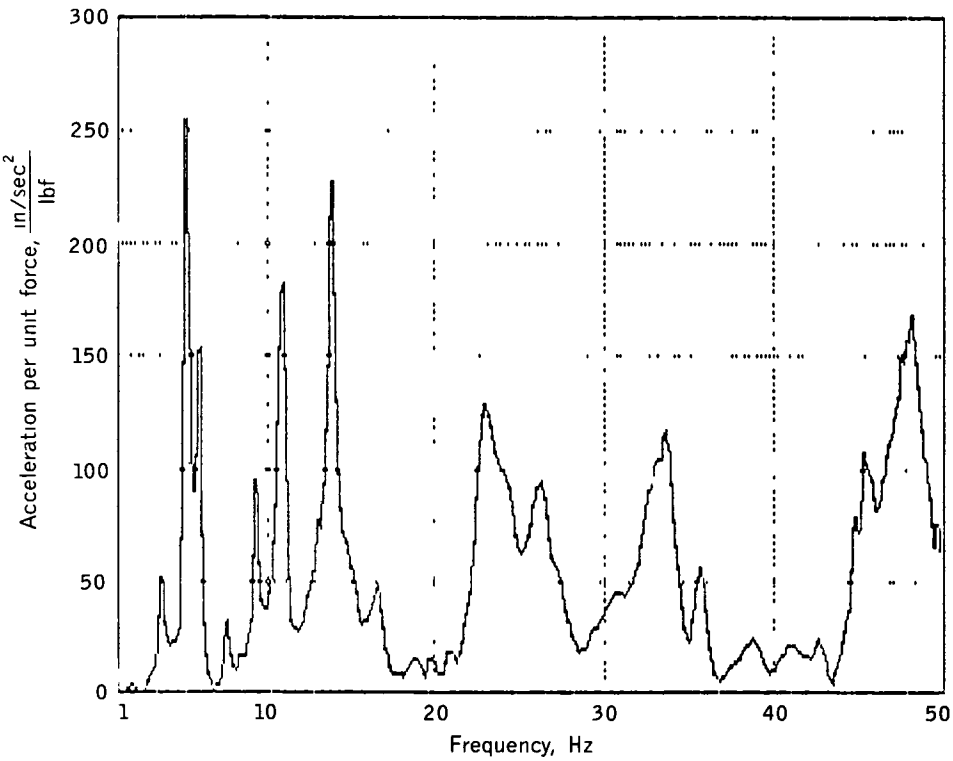

Figure B14 Right elevator (point 73) frequency response function

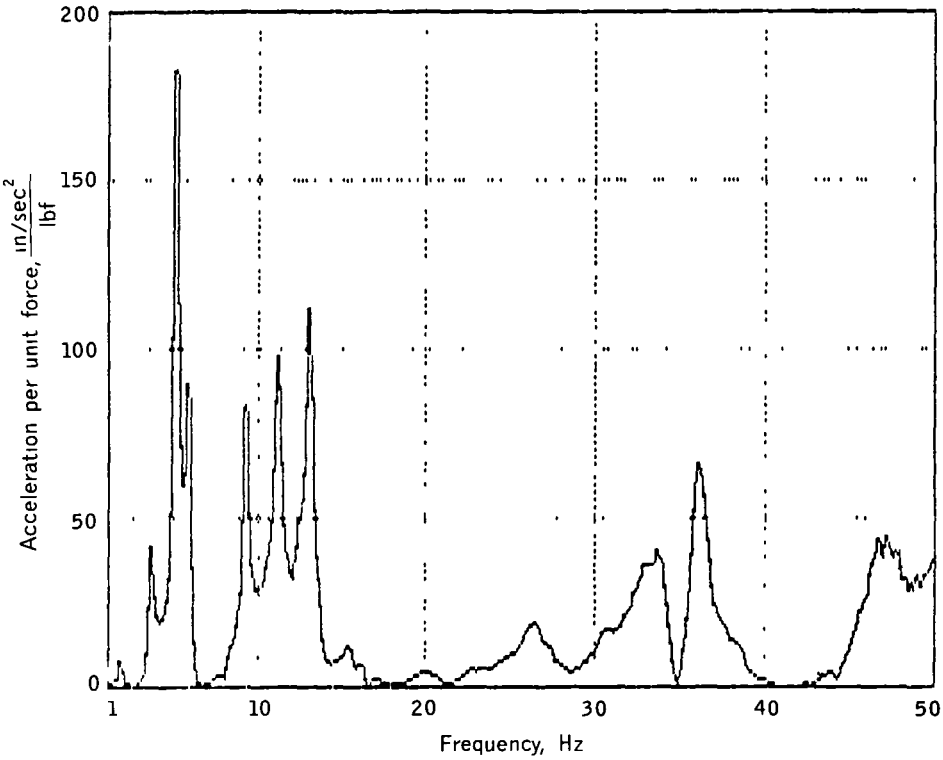

Figure B15 Vertical fin tip (point 91) frequency response

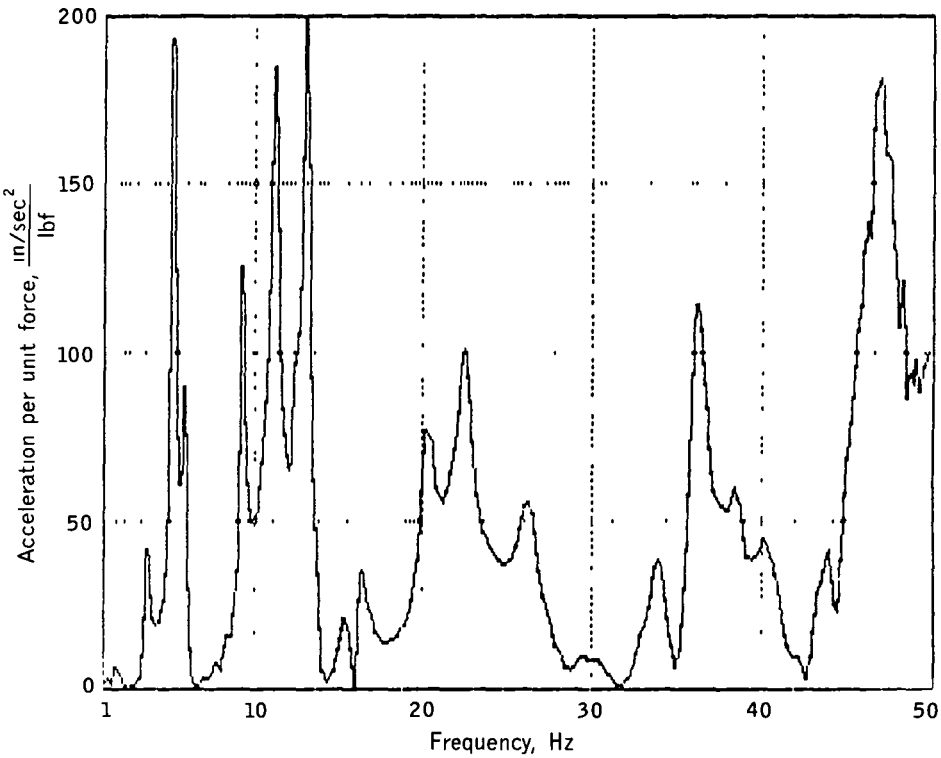

Figure B16 Rudder (point 92) frequency response function

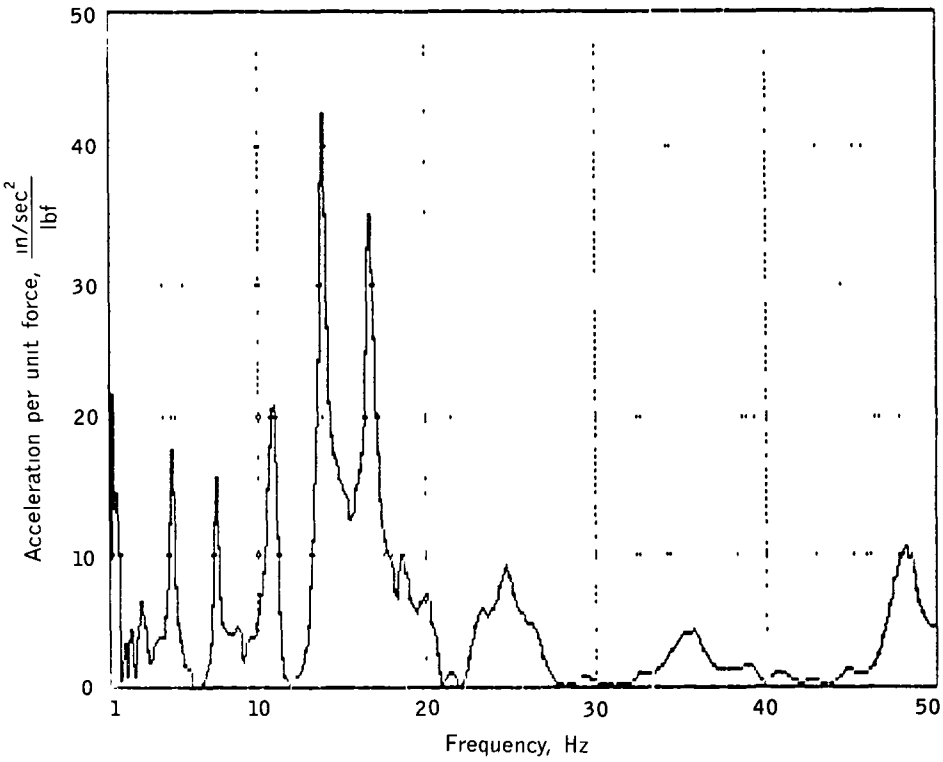

Figure B17 Forward fuselage vertical (point 75) frequency response function

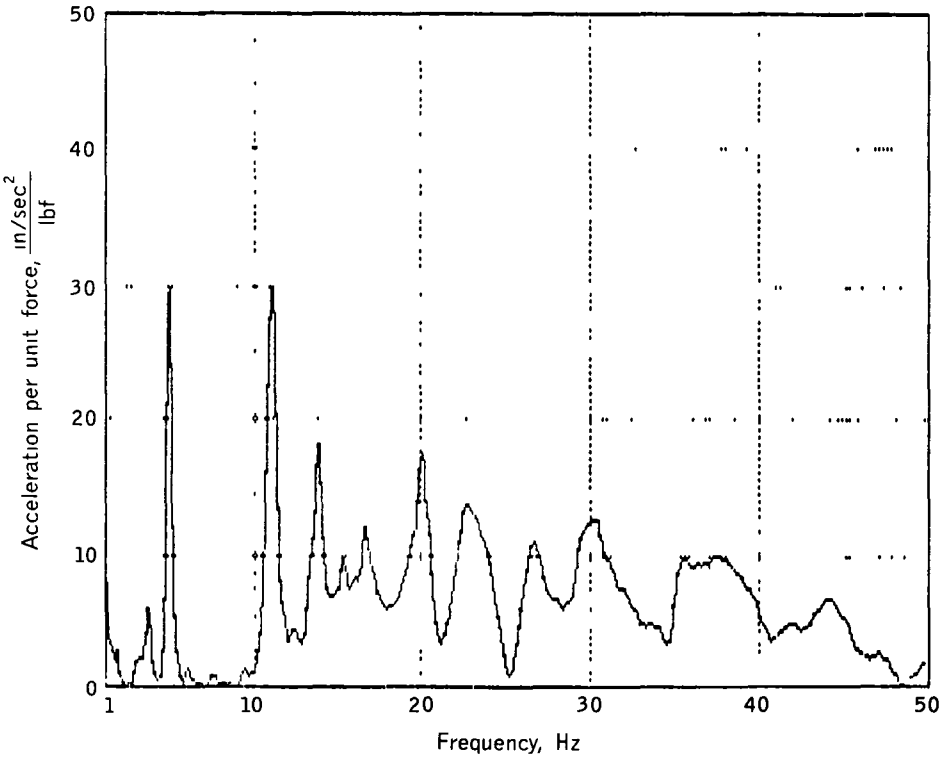

Figure B18 Aft fuselage vertical (point 82) frequency response function

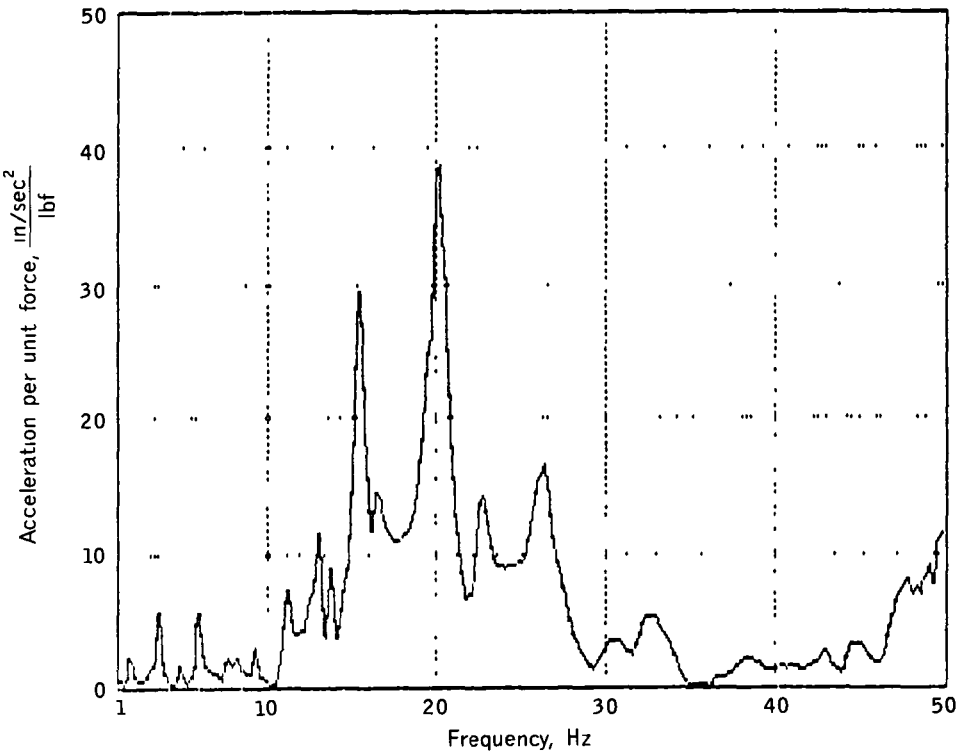

Figure B19 Forward fuselage lateral (point 75) frequency response function

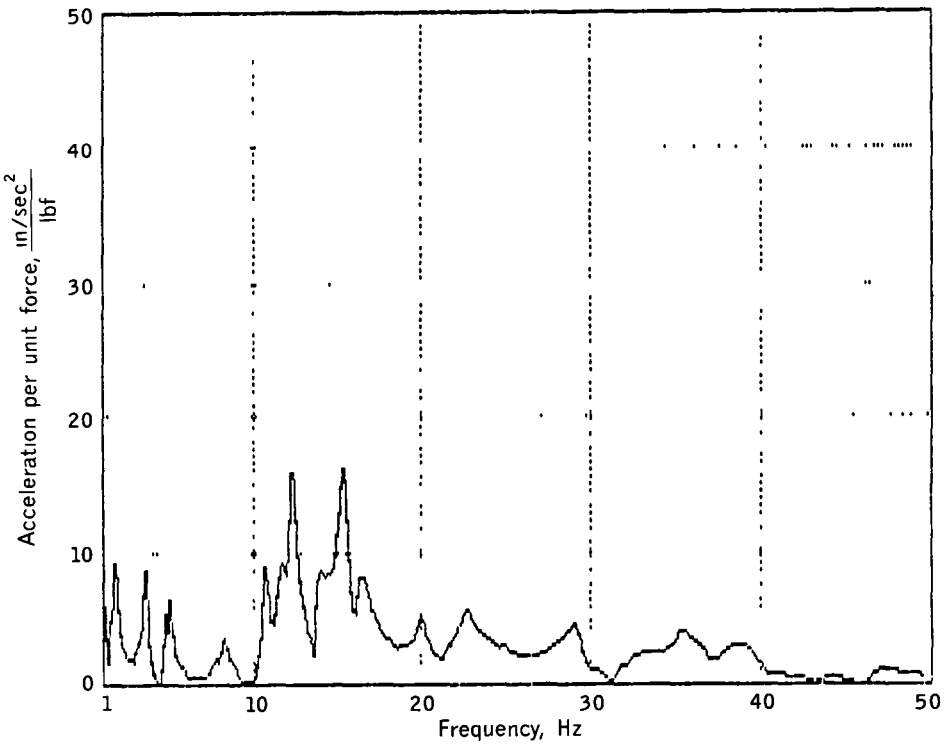

Figure B20 Aft fuselage lateral (point 82) frequency response function

Appendix C

Measured Mode-Shape Data

This appendix contains the normalized measured mode-shape data for both sine-dwell and random excitation The symmetric modes are given first (figs C1 through C7) in order of increasing frequency followed by the antisymmetric modes (figs C8 through C14) ordered in a similar manner Figures C7 and C14 give only the sine-dwell-determined modes as these modes were not obtained by the random-excitation method Figure C10 gives only the single-point-random excitation mode as this mode was not obtained during the sine-dwell test

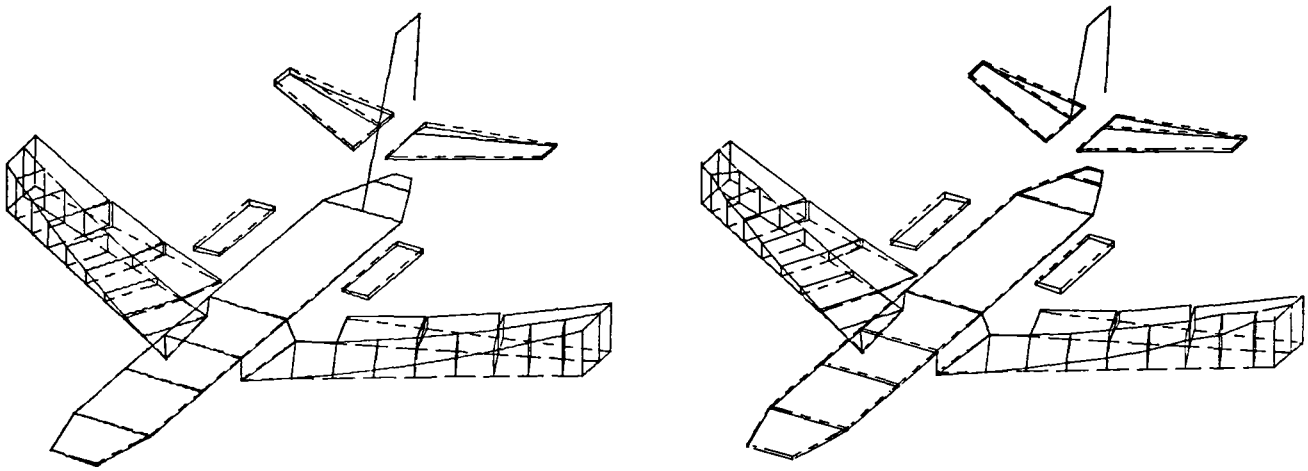

Sine-dwell excitation, frequency = 4 90 Hz

Single-point-random excitation, frequency = 4 92 Hz

Figure C1 Symmetric 1st wing bending-mode shape

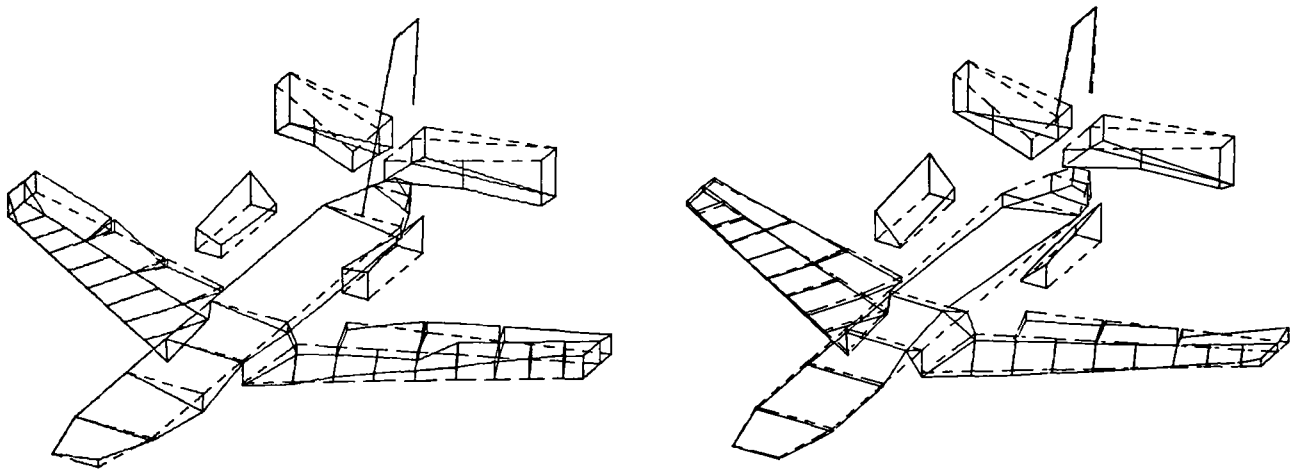

Sine-dwell excitation, frequency = 7 49 Hz

Single-point-random excitation, frequency = 7 57 Hz

Figure C2 Symmetric nacelle, wing, and stabilizer bending-mode shape

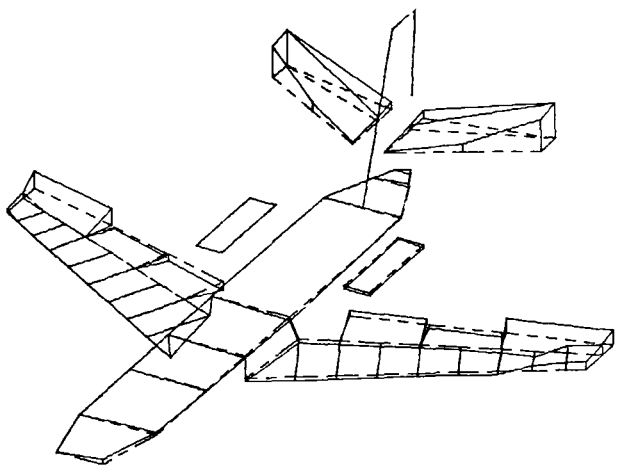

Sine-dwell excitation, frequency = 10 86 Hz

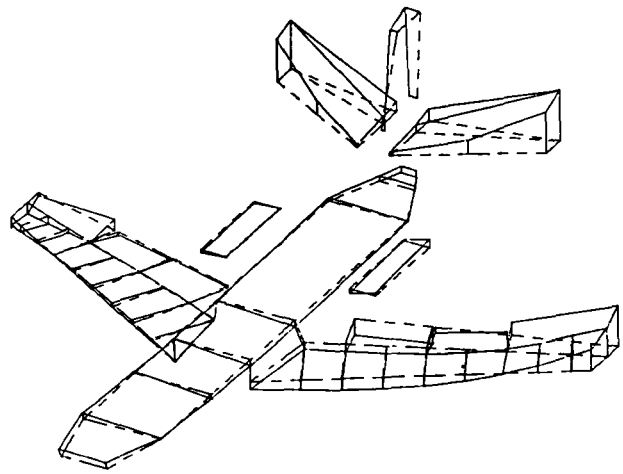

Single-point-random excitation, frequency = 10 78 Hz

Figure C3 Symmetric stabilizer and fuselage vertical bending-mode shape

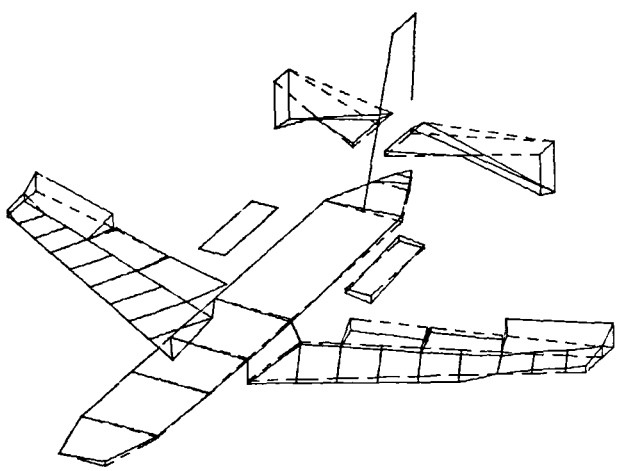

Sine-dwell excitation, frequency = 13 88 Hz

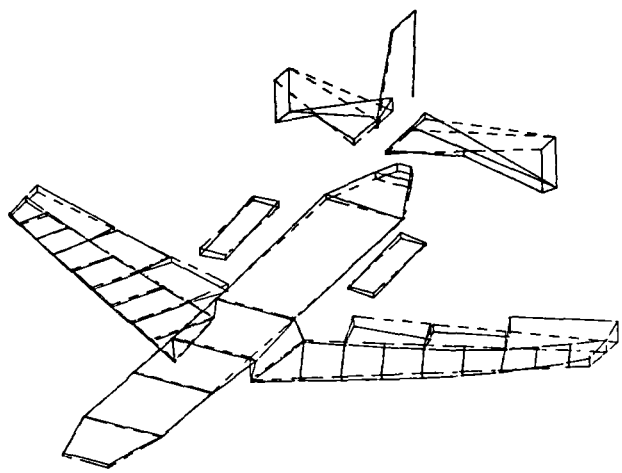

Single-point-random excitation, frequency = 13 91 Hz

Figure C4 Symmetric stabilizer and wing bending-mode shape

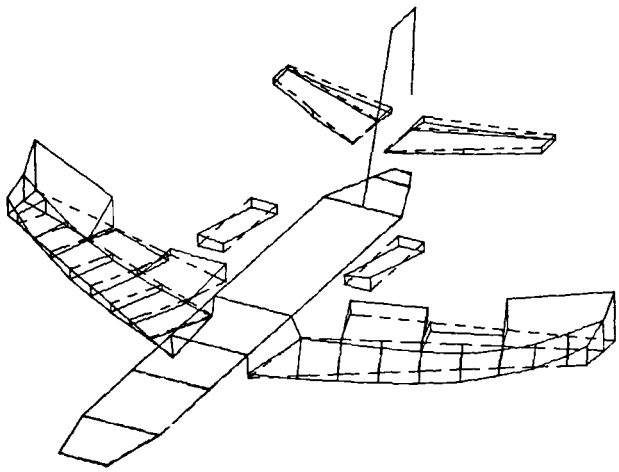

Sine-dwell excitation, frequency = 16 12 Hz

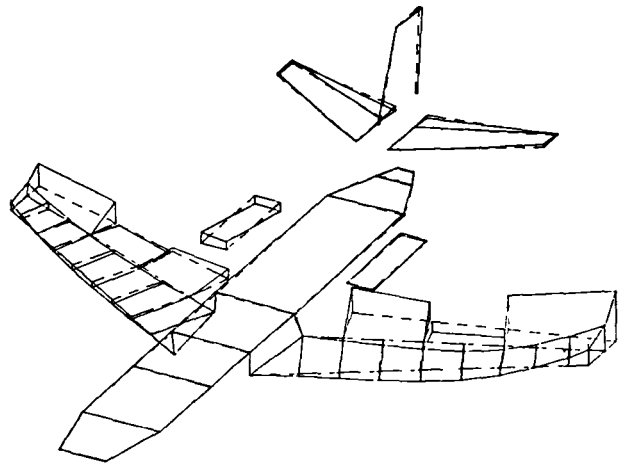

Single-point-random excitation, frequency = 16 32 Hz

Figure C5 Symmetric 2d wing bending-mode shape

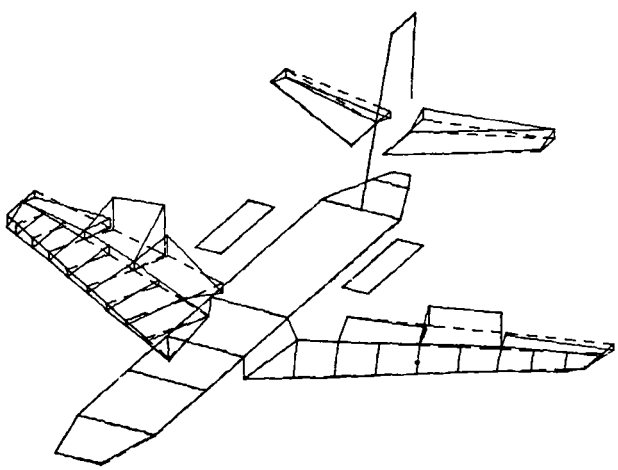

Sine-dwell excitation, frequency = 23 56 Hz

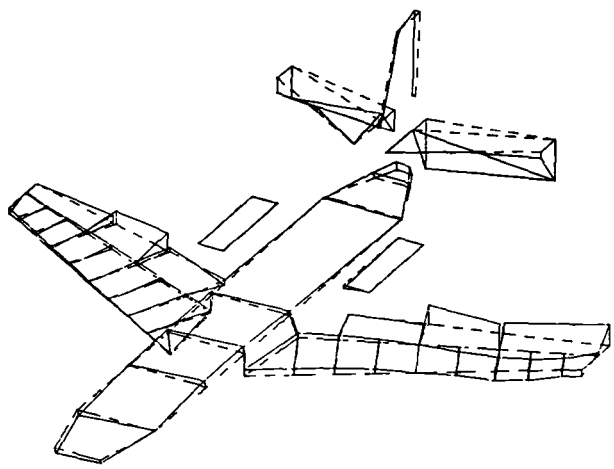

Single-point-random excitation, frequency = 24 73 Hz

Figure C6 Symmetric right wing torsion mode shape

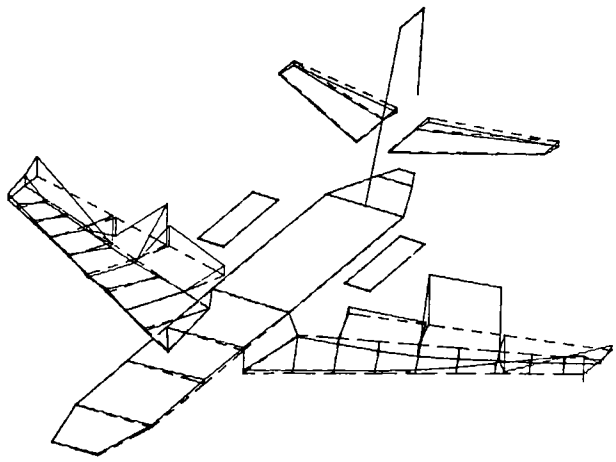

Sine-dwell excitation, frequency = 31 00 Hz

Figure C7 Symmetric left wing torsion mode shape

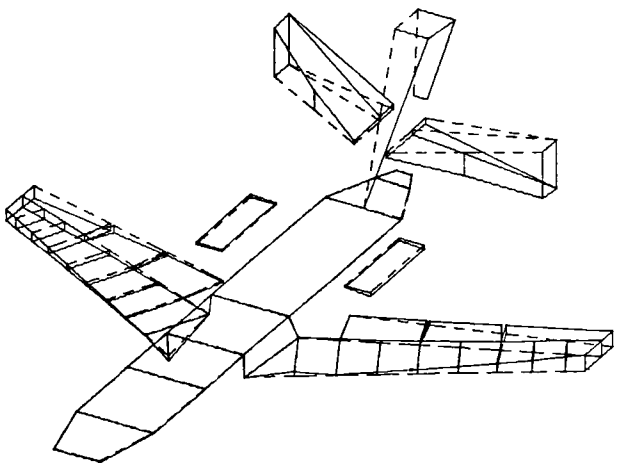

Sine-dwell excitation, frequency = 5 05 Hz

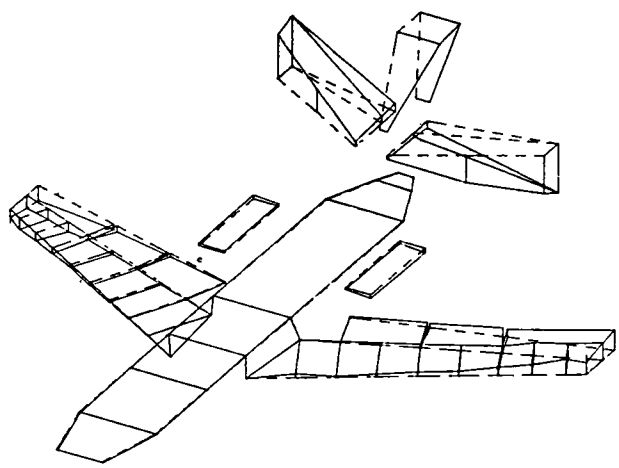

Single-point-random excitation, frequency = 5 20 Hz

Figure C8 Empennage roll and fuselage torsion mode shape

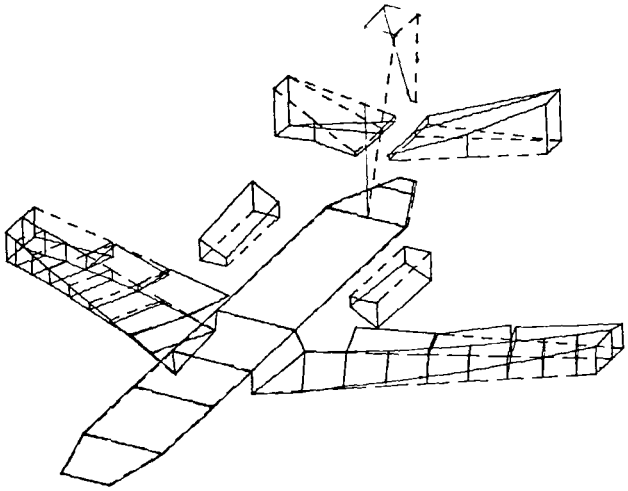

Sine-dwell excitation, frequency = 5 75 Hz

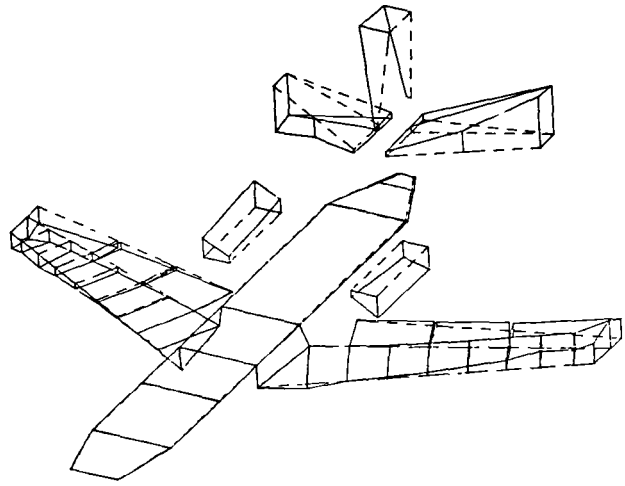

Single-point-random excitation, frequency = 5 97 Hz

Figure C9 Empennage roll, fuselage torsion, and engine pylon bending-mode shape

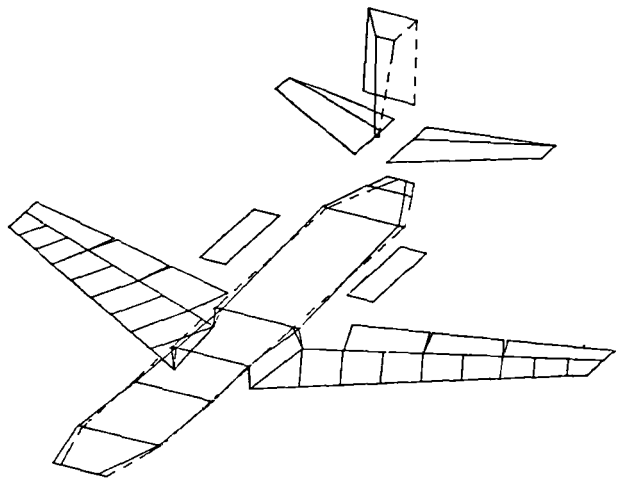

Single-point-random excitation, frequency = 7 93 Hz

Figure C10 Empennage yaw and fuselage side bending-mode shape

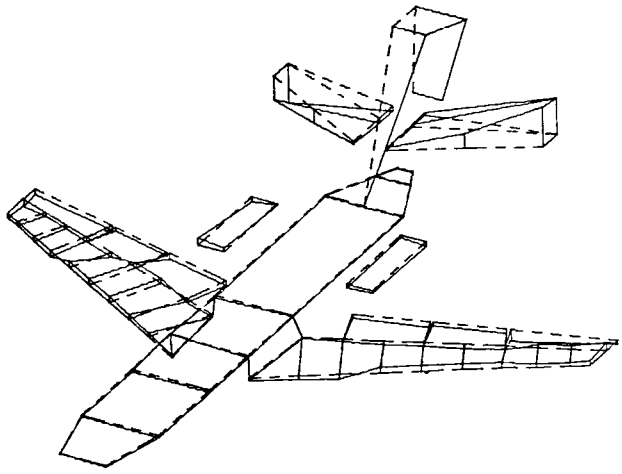

Sine-dwell excitation, frequency = 9 18 Hz

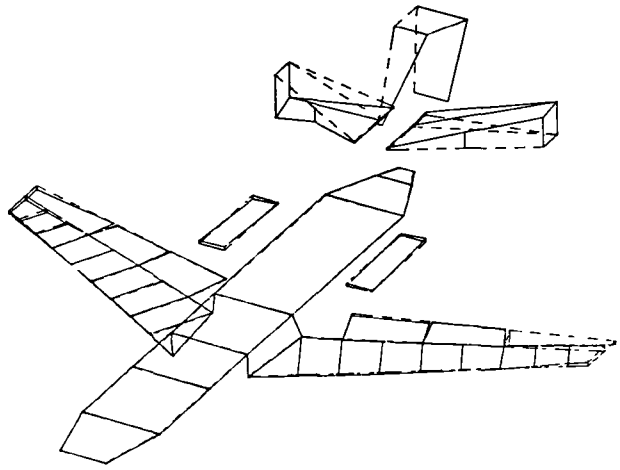

Single-point-random excitation, frequency = 9 27 Hz

Figure C11 Vertical fin bending-mode shape

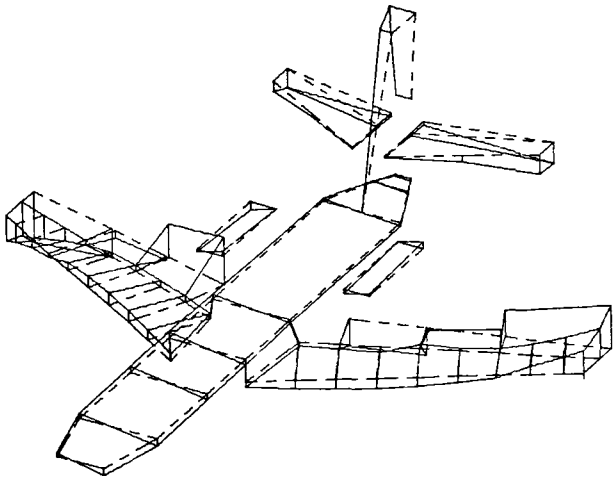

Sine-dwell excitation, frequency = 11 05 Hz

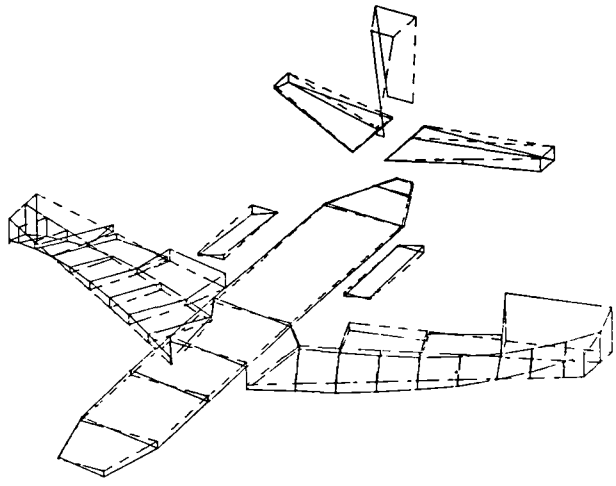

Single-point-random excitation, frequency = 11 24 Hz

Figure C12 Antisymmetric 1st wing bending-mode shape

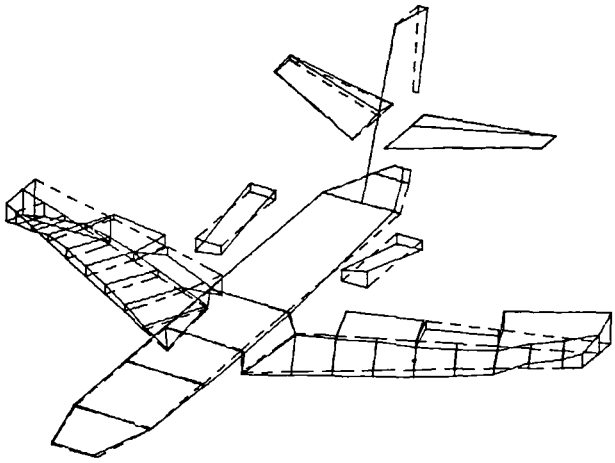

Sine-dwell excitation, frequency = 15 24 Hz

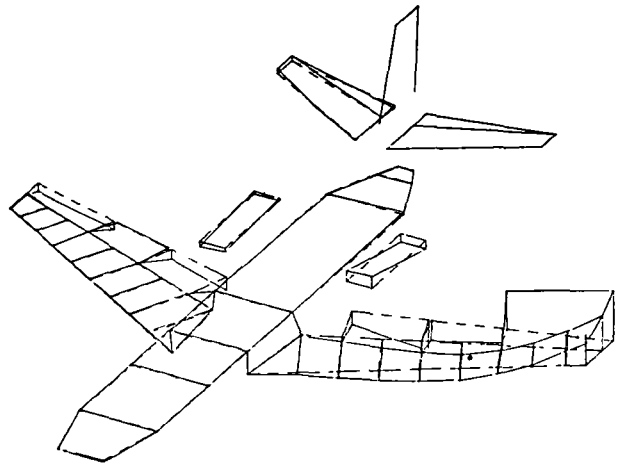

Single-point-random excitation, frequency = 15 39 Hz

Figure C13 Antisymmetric wing bending and engine pylon pitch mode shape

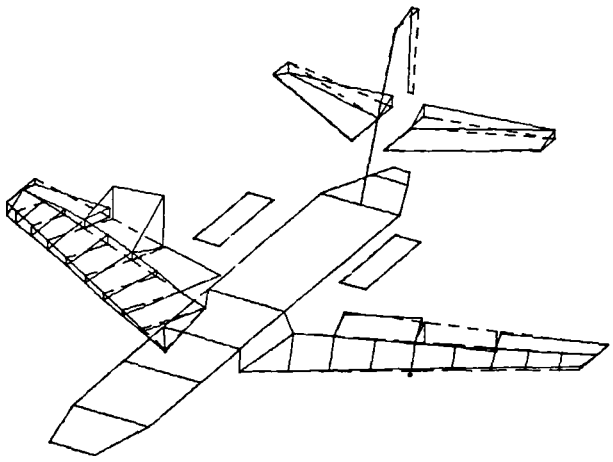

Sine-dwell excitation, frequency = 23 48 Hz

Figure C14 Antisymmetric wing torsion mode shape

References

1 Etchberger, F R , et al *LFC Leading Edge Glove Flight-Aircraft Modification Design, Test Article Development, and Systems Integration* NASA CR-172136, 1983

2 *Modal-Plus-User Manual* Structural Dynamics Research Corp , Aug 1981 (Version 6 0)

3 Richardson, Mark Modal Analysis Using Digital Test Systems *Seminar on Understanding Digital Control and Analysis in Vibration Test Systems,* Part 2, Shock and Vibration Information Center, Naval Res Lab , May 1975, pp 43-64 (Available as NASA TM X-74684)

4 Crooks, O J *Model 1329 JetStar Ground Vibration Test* Rep No ER 4220, Lockheed Aircraft Corp , Mar 31, 1961 (Rev June 15, 1961)

Standard Bibliographic Page

1 Report No	2 Government Accession No	3 Recipient's Catalog No
NASA TM-86398		

4 Title and Subtitle	5 Report Date
Ground Vibration Test of the Laminar Flow Control JetStar Airplane	October 1985
	6 Performing Organization Code: 505-33-43-07
7 Author(s): Michael W Kehoe, F W Cazier, Jr , and Joseph F Ellison	8 Performing Organization Report No: L-15949
9 Performing Organization Name and Address: NASA Langley Research Center, Hampton, VA 23665-5225	10 Work Unit No
	11 Contract or Grant No
12 Sponsoring Agency Name and Address: National Aeronautics and Space Administration, Washington, DC 20546-0001	13 Type of Report and Period Covered: Technical Memorandum
	14 Sponsoring Agency Code

15 Supplementary Notes

Michael W Kehoe and Joseph F Ellison Ames Research Center, Dryden Flight Research Facility, Edwards, California

F W Cazier, Jr Langley Research Center, Hampton, Virginia

16 Abstract

A ground vibration test was conducted on a Lockheed JetStar airplane that had been modified for the purpose of conducting laminar flow control experiments The test was performed prior to initial flight flutter tests Both sine-dwell and single-point-random excitation methods were used The data presented include frequency response functions and a comparison of mode frequencies and mode shapes from both methods

17 Key Words (Suggested by Authors(s))	18 Distribution Statement
Ground vibration tests JetStar airplane Structural dynamics	Unclassified—Unlimited Subject Category 05

19 Security Classif (of this report)	20 Security Classif (of this page)	21 No of Pages	22 Price
Unclassified	Unclassified	60	A04

For sale by the National Technical Information Service, Springfield, Virginia 22161

NASA-Langley, 1985

End of Document